Immunity
Article

The Tumor Necrosis Factor Family Receptors RANK and CD40 Cooperatively Establish the Thymic Medullary Microenvironment and Self-Tolerance

Taishin Akiyama,[1,2,*] Yusuke Shimo,[1] Hiromi Yanai,[1] Junwen Qin,[1] Daisuke Ohshima,[1] Yuya Maruyama,[1] Yukiko Asaumi,[1] Juli Kitazawa,[1] Hiroshi Takayanagi,[3] Josef M. Penninger,[4] Mitsuru Matsumoto,[5] Takeshi Nitta,[6] Yousuke Takahama,[6] and Jun-ichiro Inoue[1,*]

[1]Division of Cellular and Molecular biology, Institute of Medical Science, University of Tokyo, 4-6-1 Shirokane-dai, Minato-ku, Tokyo 108-8639, Japan

[2]Precursory Research for Embryonic Science and Technology, Japan Science and Technology Agency, 4-1-8 Honcho Kawaguchi, Saitama, 332-0012 Japan

[3]Department of Cell Signaling, Tokyo Medical and Dental University, 1-5-45 Yushima Bunkyo-ku, Tokyo 113-8549, Japan

[4]Institute of Molecular Biotechnology of the Austrian Academy Sciences, 1030 Vienna, Austria

[5]Division of Molecular Immunology, Institute for Enzyme Research

[6]Division of Experimental Immunology, Institute for Genome Research

University of Tokushima, 3-18-15 Kuramoto, Tokushima 770-8503, Japan

*Correspondence: taishin@ims.u-tokyo.ac.jp (T.A.), jun-i@ims.u-tokyo.ac.jp (J.I.)

DOI 10.1016/j.immuni.2008.06.015

SUMMARY

Medullary thymic epithelial cells (mTECs) establish T cell self-tolerance through the expression of autoimmune regulator (Aire) and peripheral tissue-specific self-antigens. However, signals underlying mTEC development remain largely unclear. Here, we demonstrate crucial regulation of mTEC development by receptor activator of NF-κB (RANK) and CD40 signals. Whereas only RANK signaling was essential for mTEC development during embryogenesis, in postnatal mice, cooperation between CD40 and RANK signals was required for mTEC development to successfully establish the medullary microenvironment. Ligation of RANK or CD40 on fetal thymic stroma in vitro induced mTEC development in a tumor necrosis factor-associated factor 6 (TRAF6)-, NF-κB inducing kinase (NIK)-, and IκB kinase β (IKKβ)-dependent manner. These results show that developmental-stage-dependent cooperation between RANK and CD40 promotes mTEC development, thereby establishing self-tolerance.

INTRODUCTION

Clonal deletion is one of the main mechanisms maintaining T cell tolerance. T cell clones that have high avidity for self-antigens are eliminated during their development in the thymus (Kyewski and Klein, 2006; Mathis and Benoist, 2004). Self-antigens are predominantly expressed and presented by thymic epithelial cells (TECs) and dendritic cells (DCs). Medullary thymic epithelial cells (mTECs) have the unique property of promiscuously expressing peripheral tissue-specific self-antigens (TSAs) (Derbinski et al., 2001). Therefore, it has been proposed that developing T cells encounter TSAs in the thymic medulla for clonal deletion (Derbinski et al., 2001; Kyewski and Klein, 2006; Mathis and Benoist, 2004). This hypothesis is supported by the study of autoimmune regulator (Aire), inactivation or deficiency of which results in autoimmune polyendocrinopathy-candidiasis ectodermal dystrophy (Aaltonen and Bjorses, 1999; Nagamine et al., 1997). Aire is preferentially expressed in mTECs, and lack of Aire in mice results in the defective expression of some TSAs (Anderson et al., 2002; Mathis and Benoist, 2004).

Even though an increasing body of evidence indicates crucial roles for mTECs in establishing self-tolerance in the thymus, signaling pathways underlying the differentiation and proliferation of mTECs expressing Aire and TSAs are poorly understood. Analyses of gene-deficient and mutant mice strongly suggest that activation of NF-κB is required for the development of mTECs (Burkly et al., 1995; Franzoso et al., 1997; Weih et al., 1995; Zhang et al., 2007). Two distinct signaling pathways, the classical and nonclassical, are thought to activate NF-κB (Bonizzi and Karin, 2004; Hoffmann and Baltimore, 2006). Previous studies indicated that NF-κB inducing kinase (NIK), IκB kinase (IKK) α, and RelB are necessary for the development of mTECs to induce self-tolerance (Burkly et al., 1995; Kajiura et al., 2004; Kinoshita et al., 2006; Weih et al., 1995), suggesting a requirement for the nonclassical NF-κB pathway in mTECs. We previously reported that TNF receptor-associated factor 6 (TRAF6), a signal transducer activating the classical NF-κB pathway and MAPK pathway (Inoue et al., 2007), also plays a crucial role (Akiyama et al., 2005), suggesting that both classical and nonclassical NF-κB activation pathways are required for the development of mTECs expressing Aire and TSAs. However, the ligand and receptors that trigger the signal to engage in the activation of NF-κBs remains unclear.

Ligation of lymphotoxin β receptor (LtβR), a member of the TNF receptor superfamily (TNFRSF), activates both classical and nonclassical NF-κB pathways. Deficiency of LtβR in the stroma compartment resulted in the reduction of *Ulex europaeus* agglutinin-1-positive (UEA-1$^+$) mTECs (Boehm et al., 2003; Venanzi et al., 2007). However, the reduction of UEA-1$^+$ mTECs in

LtβR-deficient (*Ltbr*$^{-/-}$) thymus was substantially milder than in the thymus of the alymphoplasia strain of mice (*aly/aly*) (Boehm et al., 2003), which have a dysfunctional point mutation in the *Nik* gene (Shinkura et al., 1999; Matsushima et al., 2001). These data suggested that LtβR is involved in the development of mTECs. On the other hand, deficiency in Ltα or Ltβ, which constitutes the LtβR ligand, did not affect the development of mTECs (Boehm et al., 2003; Chin et al., 2003). Involvement of the CD40 ligand (CD40L)-CD40 interaction in inducing mTECs has also been reported. Thymic overexpression of CD40 ligand resulted in a loss of the thymic cortex and an expansion of the medulla (Clegg et al., 1997; Dunn et al., 1997). Flow-cytometric analysis of CD40 ligand (CD40L)-deficient mice (*Cd40lg*$^{-/-}$) revealed that the subset of mTECs expressing relatively low levels of MHC class II was reduced in the thymus (Gray et al., 2006). However, immunohistochemical study indicated no apparent defect in the medullary organization of *Cd40lg*$^{-/-}$ thymi (Dunn et al., 1997). It has also recently been reported that receptor activator of NF-κB (RANK)-deficient mice (*Tnfrsf11a*$^{-/-}$) exhibits a severe reduction in CD80^{+} and Aire^{+} mTECs at 4 to 6 weeks of age (Rossi et al., 2007). However, no defects in medullary organization or development of keratin-5^{+} mTECs were observed in *Tnfrsf11a*$^{-/-}$ mice (Rossi et al., 2007). Importantly, the defects of *Ltbr*$^{-/-}$, *Cd40lg*$^{-/-}$, or *Tnfrsf11a* $^{-/-}$ mouse lines in establishing the thymic medullary microenvironment appear to be substantially milder compared with mutant mice deficient in the NF-κB activation pathway such as TRAF6-deficient (*Traf6*$^{-/-}$), *aly/aly*, or RelB-deficient (*Relb*$^{-/-}$) mice (Akiyama et al., 2005; Burkly et al., 1995; Kajiura et al., 2004; Weih et al., 1995).

Here we demonstrate cooperation between RANK and CD40 as a critical event in mTEC development essential for self-tolerance. Through extensive analyses of RANK-ligand-deficient mice (*Tnfsf11*$^{-/-}$), *Cd40*$^{-/-}$, and *Tnfsf11*$^{-/-}$*Cd40*$^{-/-}$ mice and of fetal thymic stroma stimulated in vitro by RANK ligand (RANKL) and CD40L, we established that RANKL-RANK signaling plays crucial roles in the development of mTECs expressing UEA-1 ligand, Aire, and TSAs during embryogenesis. However, after birth, cooperation of CD40L-CD40 and RANKL-RANK signaling is required for the development of mTECs, which are necessary for the formation of an intact medullary microenvironment.

RESULTS

RANKL Is Essential for the Generation of mTECs in Embryonic Thymus

We previously reported a requirement for TRAF6 in the development of mature mTECs and the control of thymic-stroma-dependent self-tolerance (Akiyama et al., 2005). Fetal thymic organ cultures treated with 2-deoxyguanosine (2-DG FTOC), in which lymphocytes are eliminated, developed into thymi with intact microenvironments after grafting in nude mice. However, 2-DG FTOC prepared from *Traf6*$^{-/-}$ at embryonic day 14 (E14) failed to develop mTECs (Akiyama et al., 2005). This result implied that receptors upstream of TRAF6 necessary for developing mTECs are present in embryonic thymic stroma. We therefore tried to determine the ligand and receptor system that mediates mTEC development via TRAF6 signal transduction. Because TRAF6 transduces signals from various members of the TNF receptor superfamily, we investigated the expression profile in 2-DG FTOC by RT-PCR analysis (data not shown). One of the candidates obtained by this assay was RANK; it has previously been reported that the RANKL-RANK-TRAF6 signaling axis is essential for osteoclastogenesis and lymph node organogenesis (Theill et al., 2002; Kobayashi et al., 2001; Yoshida et al., 2002). To address this issue, we analyzed thymic cryosections of RANKL-deficient (*Tnfsf11*$^{-/-}$) mice at E14, E16, and E18 by immunostaining to detect keratin-5 and UEA-1, markers for mTECs (Figure 1A). The generation of mTECs expressing UEA-1 ligand in embryonic thymus was strictly dependent on RANKL. The deficiency in mTECs was comparable to that observed in *Traf6*$^{-/-}$ embryos (Akiyama et al., 2005). Aire^{+} cells and EpCAM^{+} cells were also abolished in E18 *Tnfsf11*$^{-/-}$ thymic sections (Figure 1B). Quantitative and semiqunatitative RT-PCR analyses confirmed the severe reduction in *Aire* expression in *Tnfsf11*$^{-/-}$ embryo (Figure 1C and Figure S1, available online). Moreover, we found that the expression of both Aire-dependent (*Sap1*) and Aire-independent TSAs (*Crp*, *Gad 67*) were severely reduced in embryonic thymi of *Tnfsf11*$^{-/-}$ mice (Figure 1D and Figure S1). When RANK-Fc was added, the development of mature mTECs was markedly impaired in FTOC as judged from the severe reduction of UEA-1^{+} cells (Figure 1E), strongly suggesting that RANKL-RANK interaction in embryonic thymus, but not in other organs, is required for development of mTECs. Overall, these data suggest that RANKL-RANK interaction in embryonic thymus is essential for the generation of mTECs expressing Aire and TSAs.

RANKL Signal Partially Contributes to the Development or Maintenance of mTECs in Postnatal Thymus

Interestingly, the expression of UEA-1-ligand, Aire, and EpCAM in the thymic medulla became apparent at postnatal day 3 (PN3) even in the absence of RANKL (Figures 1A and 1B). This observation implied that, after birth, another molecule is capable of replacing the RANKL signal required for the development of mTECs. During perinatal development, several dynamic changes, such as completion of medullary organization and differentiation of large numbers of single-positive thymocytes, occur in the thymus. Such changes may affect RANKL dependency in the development of mTECs. In order to investigate the function of RANKL signaling in postnatal thymus, we analyzed thymi of 2-week-old *Tnfsf11*$^{-/-}$ mice. Cortico-medullar junctions appeared to be normal in paraffin-embedded thymic sections of *Tnfsf11*$^{-/-}$ mice (Figure 2A). Immunohistochemical staining of cryosections with keratin-5 and CD8α-antibodies revealed proper localization of mTECs in the medulla of 2-week-old *Tnfsf11*$^{-/-}$ thymi (Figure 2A). These findings were consistent with previous histological observations (Kong et al., 1999). However, *Tnfsf11*$^{-/-}$ thymi displayed a marked reduction in the number of cells expressing mTEC markers such as UEA-1 ligand and Claudin-3 and -4 (Cld3,4) (Hamazaki et al., 2007), or ER-TR5 (Figure 2A). Quantitative and semiquantitative RT-PCR analysis further showed a reduction in the expression of *Aire* and TSA mRNAs in *Tnfsf11*$^{-/-}$ thymi (Figure 2B and Figure S1). Moreover, immunohistochemical analysis indicated that the number of Aire^{+} mTECs was severely decreased in *Tnfsf11*$^{-/-}$ thymi (Figure 2C). The severe reduction in Aire-expressing mTECs in *Tnfsf11*$^{-/-}$ mice is consistent with previous results in *Rank*$^{-/-}$

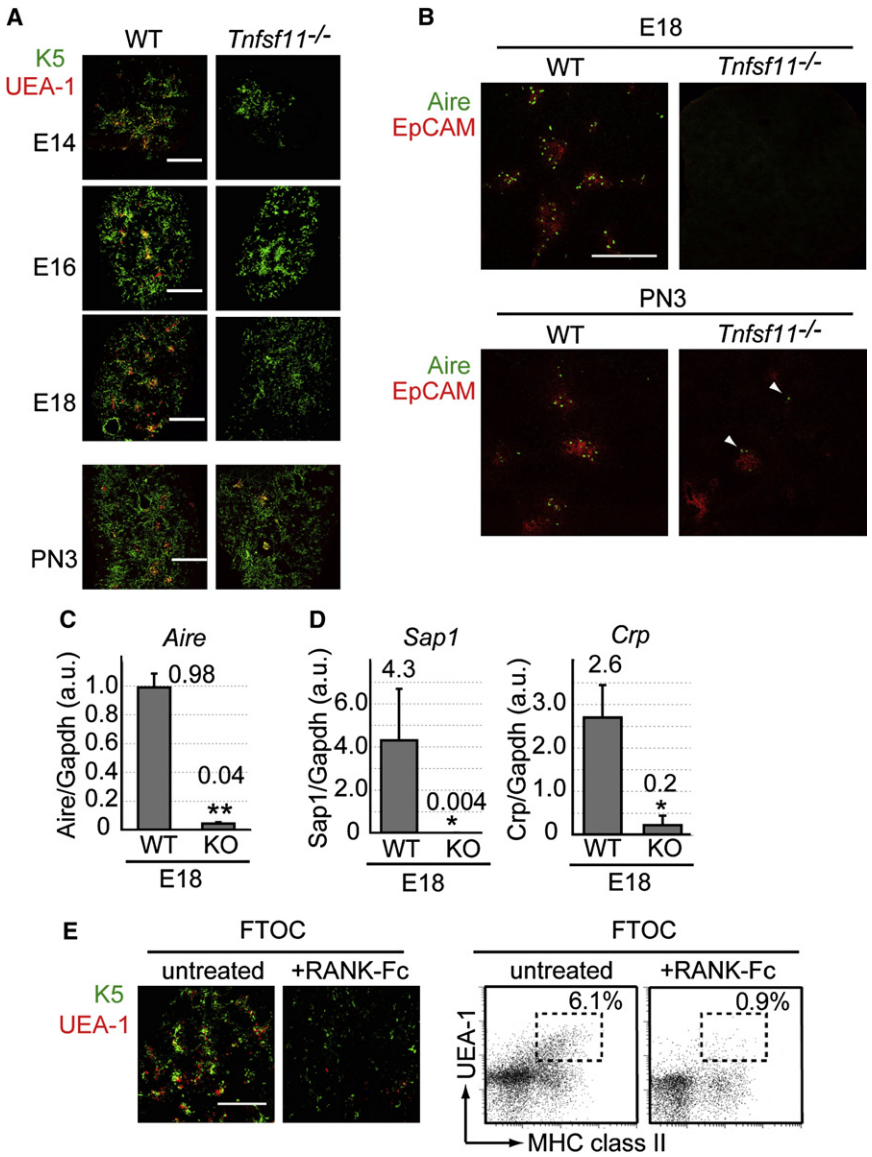

Figure 1. RANKL Signal Is Essential for the Development of mTECs Expressing UEA-1 Ligand, Aire, and TSAs in Embryos

(A) Immunohistochemical staining of thymic cryosections of *Tnfsf11*$^{-/-}$ at embryonic day 14 (E14), 16 (E16), and 18 (E18), and postnatal day 3 (PN3) with a combination of keratin-5 antibody (green) and UEA-1 (red). Scale bars represent 200 μm.

(B) Immunohistochemical staining of thymic cryosections of *Tnfsf11*$^{-/-}$ at E18 with a combination of Aire antibody (green) and EpCAM antibody (red). Arrowheads indicate Aire-positive cells.

(C) Real-time PCR analysis of the expression of *Aire* in wild-type or *Tnfsf11*$^{-/-}$ E18 thymus. Asterisks indicate that the difference is statistically significant (**$p < 0.01$, Student's t test). Values are arbitrary units (a.u.) normalized to *GAPDH*. Error bars represent one standard deviation (SD) above the mean (indicated above the bars) of at least three independent experiments.

(D) Real-time PCR analysis of the expression of TSAs (*Sap1* and *Crp*) in wild-type or *Tnfsf11*$^{-/-}$ E18 thymus. Asterisks indicate that the difference is statistically significant (*$p < 0.05$, Student's t test) Values are arbitrary units normalized to *GAPDH*.

(E) Development of mTECs in FTOC is blocked by the addition of RANK-Fc. Fetal thymus was cultured in the presence or absence of RANK-Fc for 4 days. Left panels exhibit immunohistochemical staining of the FTOC with a combination of anti-keratin-5 (green) and UEA-1 (red). Right panels show flow-cytometric analysis of the FTOC. Collagenase-treated FTOC cell suspensions were stained with UEA-1, anti-MHC class II (I-A/I-E), anti-CD45, and TER119 antibody and analyzed with a flow cytometer. Fraction of MHC class II^{+} UEA-1^{+} cells (gated on CD45-negative cells) was decreased. Data is a typical example from two independent experiments.

mice. RANK is the only functional receptor for RANKL known to activate intracellular signaling. Therefore, these data suggested that the RANKL-RANK interaction contributes to establishing the medullary microenvironment in the postnatal thymus. However, it should be noted that the mTEC defect in 2-week-old *Tnfsf11*$^{-/-}$ mice is milder than that in TRAF6-deficient (*Traf6*$^{-/-}$) mice, RelB-deficient (*Relb*$^{-/-}$) mice, or *aly/aly* mice at the same ages. Thymi of these latter mutant mice show severe defects in thymic medullary organization, such as undefined cortico-medullar junctions, scattered distribution of keratin-5^{+} cells, and severe reduction in mTECs expressing UEA-1-ligand, Cld3,4, Aire, and TSAs (Akiyama et al., 2005; Burkly et al., 1995; Kajiura et al., 2004; Miyawaki et al., 1994; Weih et al., 1995).

Double Deficiency in RANKL and CD40 Impairs the Postnatal Development of mTECs

As described above, previous studies suggested that LtβR and, at least in part, CD40 are involved in the development or maintenance of mTECs (Boehm et al., 2003; Gray et al., 2006; Venanzi et al., 2007). Semiquantitative expression analysis of the TNFRSF revealed the expression of both LtβR and CD40 in 2-DG FTOC (data not shown). We have recently demonstrated that TRAF6 is dispensable for NF-κB activation induced by ligation of LtβR (Qin et al., 2007), whereas TRAF6 is involved in classical NF-κB activation induced by CD40 ligation (Ishida et al., 1996; Kobayashi et al., 2004). Furthermore, semiquantitative RT-PCR analysis revealed expression of CD40 ligand (CD40L) mRNA in thymus at E17 at the earliest. CD40L expression reached plateau after birth (Figure S2), which is consistent with previous immunohistochemical studies (Dunn et al., 1997). In addition, our immunohistochemical analyses showed the expressions of both RANK and CD40 in adult thymic medulla (Figure S3). On the basis of these observations, we hypothesized that CD40L-CD40 signals emerge in the thymic medulla just before birth and that such signals can compensate for RANKL-RANK deficiency in the postnatal thymus.

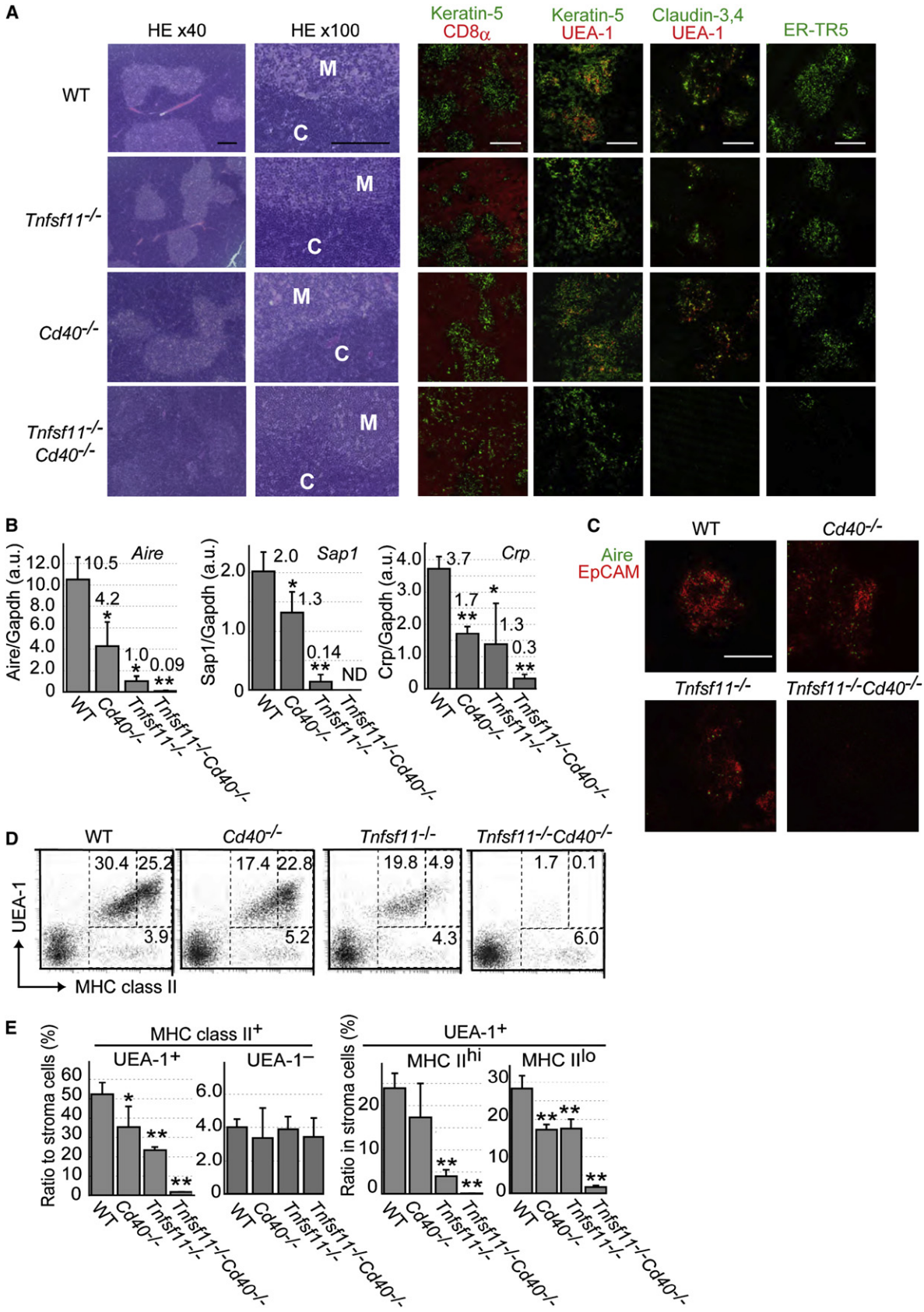
A
HE x40
HE x100
Keratin-5 CD8α
Keratin-5 UEA-1
Claudin-3,4 UEA-1
ER-TR5
WT
Tnfsf11-/-
Cd40-/-
Tnfsf11-/- Cd40-/-
M
C
B
Aire/Gapdh (a.u.)
Sap1/Gapdh (a.u.)
Crp/Gapdh (a.u.)
Aire
Sap1
Crp
ND
WT
Cd40-/-
Tnfsf11-/-
Tnfsf11-/-Cd40-/-
C
Aire
EpCAM
WT
Cd40-/-
Tnfsf11-/-
Tnfsf11-/-Cd40-/-
D
UEA-1
MHC class II
30.4
25.2
3.9
17.4
22.8
5.2
19.8
4.9
4.3
1.7
0.1
6.0
E
Ratio to stroma cells (%)
Ratio in stroma cells (%)
MHC class II+
UEA-1+
UEA-1−
UEA-1+
MHC IIhi
MHC IIlo

We then investigated the thymic architecture of CD40-deficient mice (*Cd40*$^{-/-}$). At E14, thymi of *Cd40*$^{-/-}$ mice showed normal development of UEA-1^{+} mTECs (data not shown), which was consistent with the lack of CD40L expression in the embryonic thymus. Furthermore, histological and immunohistochemical studies revealed that 2-week-old *Cd40*$^{-/-}$ mice did not show any appreciable differences in the development and distribution of mTECs from wild-type control (Figure 2A), an observation consistent with previous immunohistochemical analyses on *Cd40lg*$^{-/-}$ mice (Dunn et al., 1997). To investigate mTEC development in more detail, whole thymic cell suspensions were prepared and assayed by flow cytometry (Figure 2D). Even if the number of mTECs was not statistically reduced as reported (Hikosaka et al., 2008, this issue of *Immunity*), the ratio of MHC class II^{+} (I-A and I-E) and UEA-1^{+} mTECs, especially the MHC class II^{lo} subset, was reduced in thymic stroma of 2-week-old *Cd40*$^{-/-}$ mice (Figures 2D and 2E). This *Cd40*$^{-/-}$ phenotype is consistent with recent flow-cytometric analysis on *Cd40lg*$^{-/-}$ mice, in which MHC class II^{lo} mTECs were reduced (Gray et al., 2006). Quantitative real-time PCR analysis revealed that expression of *Aire* and of Aire-dependent (*Sap1*) and Aire-independent (*Crp* and *Gad67*) TSAs was reduced in *Cd40*$^{-/-}$ mice as compared with wild-type mice (Figure 2D). These results indicated that CD40 contributes to the development or maintenance of mTECs after birth. Flow-cytometric analysis also revealed that single deficiency in RANKL caused a substantial reduction in MHC class II^{+} UEA-1^{+} mTECs. The reduction in the MHC class II^{hi} subset is greater than in the MHC class II^{lo} subset. However, the reduction in total UEA-1^{+} cells resembled that in CD40$^{-/-}$ mice (Figures 2D and 2E). Together with previous studies on *Tnfrsf11a*$^{-/-}$ (Rossi et al., 2007) and *CD40lg*$^{-/-}$ mice (Gray et al., 2006), our analyses on *Tnfsf11*$^{-/-}$ and *Cd40*$^{-/-}$ mice show that both RANKL-RANK and CD40L-CD40 signals partially contribute to the postnatal establishment of the intact thymic microenvironment.

Because TRAF6 and NIK transduce signals from both RANK and CD40, we hypothesized that RANKL-RANK and CD40L-CD40 may cooperatively regulate the medullary organization of the postnatal thymus. To address this issue, we generated *Tnfsf11*$^{-/-}$ *Cd40*$^{-/-}$ double-deficient mice. Strikingly, 2-week-old *Tnfsf11*$^{-/-}$ *Cd40*$^{-/-}$ mice showed severe disorganization of thymic medullary architecture. Histological and immunohistochemical analyses revealed the cortico-medullar junction to be undefined and keratin-5^{+} cells to be dispersed throughout the whole thymus of *Tnfsf11*$^{-/-}$ *Cd40*$^{-/-}$ mice (Figure 2A). Immunohistochemical staining with several mTEC markers such as UEA-1, Claudine-3,4, ER-TR5, and EpCAM further showed that the development of mTECs was almost completely abolished in the thymus of *Tnfsf11*$^{-/-}$*Cd40*$^{-/-}$ mice (Figure 2A and Figure S4). On the other hand, the development of cTECs as judged by staining with a keratin-8 antibody appeared to be normal in the thymus of *Tnfsf11*$^{-/-}$*Cd40*$^{-/-}$ mice (Figure S4). Consistent with this immunohistochemical analysis (Figure 2A), *Tnfsf11*$^{-/-}$ *Cd40*$^{-/-}$ mice showed severe reduction in MHC class II^{+}UEA-1^{+} mTECs as determined by flow-cytometric analysis (Figures 2D and 2E). On the other hand, MHC class II^{+}UEA-1^{-} stroma cell subsets that mainly included cTECs were not affected by deficiency in RANKL and CD40 (Figures 2D and 2E). Immunohistochemical and RT-PCR analyses indicated that the development of Aire^{+} mTECs and the expression of *Aire* and TSAs (*Sap1*, *Crp*, and *Gad67*) were also severely reduced in *Tnfsf11*$^{-/-}$ *Cd40*$^{-/-}$ mice as compared to wild-type, *Tnfsf11*$^{-/-}$, and *Cd40*$^{-/-}$ single-mutant mice (Figures 2B and 2C, and Figure S1). These findings strongly suggested that RANKL-RANK and CD40L-CD40 signals cooperatively regulate the development of the medullary microenvironment and mTEC maturation in the postnatal thymus.

Splenocytes from *Tnfsf11*$^{-/-}$ and *Tnfsf11*$^{-/-}$*CD40*$^{-/-}$ Mice Are Capable of Inducing Autoimmunity in Nude Mice

Several studies suggest that mature mTECs play a crucial role in establishing self-tolerance (Anderson et al., 2007) (Akiyama et al., 2005). We therefore asked whether deficiency in RANKL-RANK interaction and/or CD40L-CD40 interaction breaks self-tolerance. Even though some *Tnfsf11*$^{-/-}$ and *Tnfsf11*$^{-/-}$ *CD40*$^{-/-}$ mice exhibited weak cellular infiltration in lung and liver (data not shown) at 2 to 3 weeks of age, the infiltrations were significantly milder than in *Traf6*$^{-/-}$, *Relb*$^{-/-}$, or *aly/aly* mice (data not shown). We suspected that, because RANKL-RANK and CD40L-CD40 interactions are involved in activation of acquired immune systems such as survival and activation of

Figure 2. Effect of Deficiency of RANKL-RANK and CD40L-CD40 Signals on Thymic Medullary Microenvironment in 2-Week-Old Mice

(A) Disruption of the thymic medullary microenvironment in 2-week-old *Tnfsf11*$^{-/-}$*Cd40*$^{-/-}$, *Tnfsf11*$^{-/-}$, *Cd40*$^{-/-}$, or wild-type control mice. Paraffin-embedded thymic sections were stained with hematoxylin and eosin (left panels: 40× magnification, scale bars represent 200 μm; lower panels: 100× magnification, scale bars represent 80 μm). For the right panels, thymic cryosections of *Tnfsf11*$^{-/-}$*Cd40*$^{-/-}$ or *Cd40*$^{-/-}$ mice were stained with a combination of anti-keratin-5 (green) and anti-CD8α (red), anti-keratin-5 (green) and UEA-1 (red), anti-Cld3,4 (green) and UEA-1 (red), or anti-ER-TR5 (green). Scale bars represent 200 μm.

(B) Real-time PCR analysis of the expression of *Aire* and TSAs (*Sap1* and *Crp*) in *Tnfsf11*$^{-/-}$*Cd40*$^{-/-}$, *Cd40*$^{-/-}$, *Tnfsf11*$^{-/-}$, or wild-type control thymus at PN14 to PN16. Values are arbitrary units normalized to *GAPDH*. Error bars represent 1 SD abovethe mean (indicated above the bars) of three independent experiments. Asterisks indicate that the reduction in expression from the wild-type control is statistically significant ($p < 0.05$, Student's t test, n = 3 for each sample). Values are arbitrary units normalized to *GAPDH*.

(C) Immunohistochemical staining of thymic cryosections of *Tnfsf11*$^{-/-}$*Cd40*$^{-/-}$, *Tnfsf11*$^{-/-}$, *Cd40*$^{-/-}$, or wild-type control mice with a combination of Aire antibody (green) and EpCAM antibody (red).

(D) Flow-cytometric analysis of thymic stromal cells. Thymic cell suspensions were stained with UEA-1, anti-MHC class II (I-A/I-E), anti-CD45, and TER119 antibodies and analyzed with a flow cytometer. A subset of MHC class II^{hi} in UEA-1^{+} cells (gated on CD45- and TER119-negative cells) is labeled as "High," and a subset of MHC class II^{lo} in UEA-1^{+} cells is labeled as "Low" in the figure. Data are representative of at least four independent experiments.

(E) Summary in the ratios of TECs (subsets of UEA-1^{+} MHC class II^{+} and UEA-1^{-} MHC class II^{+}) and mTECs (subsets of UEA-1^{+} MHC class II^{hi} and UEA-1 MHC class II^{lo}) in thymic stromal cells (gated on CD45^{-} and TER119^{-}) of wild-type, *Cd40*$^{-/-}$, *Tnfsf11*$^{-/-}$, or *Tnfsf11*$^{-/-}$*Cd40*$^{-/-}$ thymus at PN14 to PN16. Asterisks indicate that the reduction from the wild-type control is statistically significant (*$p < 0.05$ and **$p < 0.01$, Student's t test; n = 6 for wild-type mice, n = 4 for *Cd40*$^{-/-}$ mice, n = 4 for *Tnfsf11*$^{-/-}$ mice, and n = 5 for *Tnfsf11*$^{-/-}$*Cd40*$^{-/-}$ mice in the Balb/c background). Error bars represent 1 SD above the mean of three independent experiments.

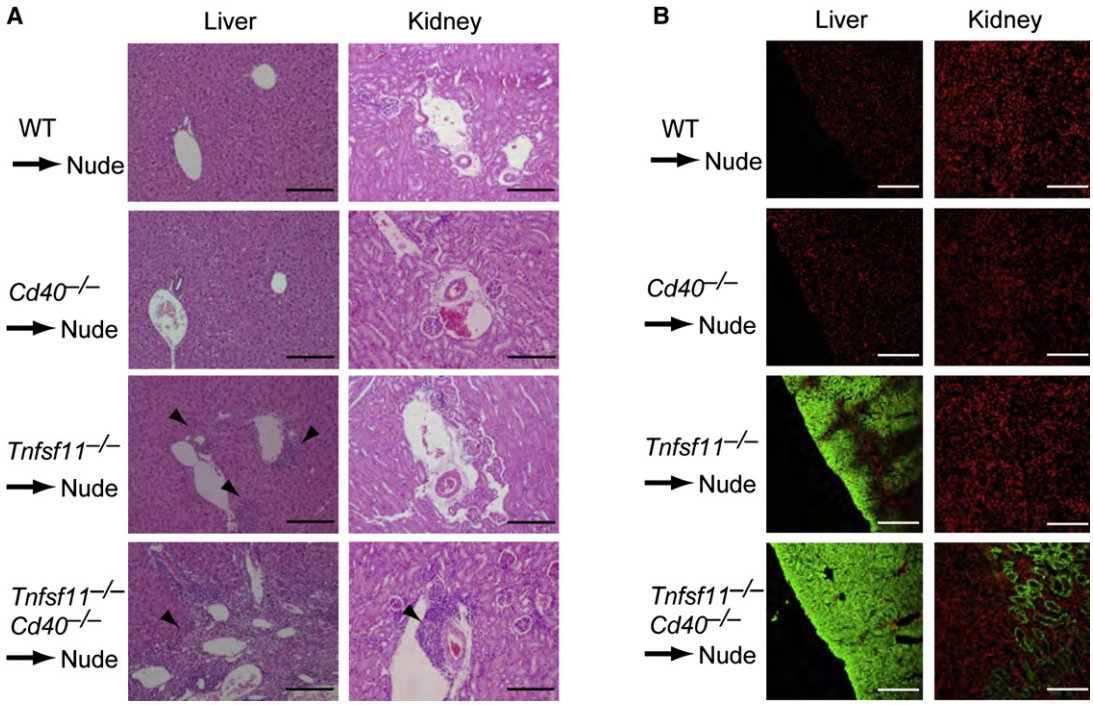

Figure 3. Transfer of Splenocytes from 2-Week-Old *Tnfsf11*$^{-/-}$ and *Tnfsf11*$^{-/-}$*Cd40*$^{-/-}$ Mice Induces Autoimmunity in Nude Mice

(A) Transfer of splenocytes from 2-week-old *Tnfsf11*$^{-/-}$ and *Tnfsf11*$^{-/-}$*Cd40*$^{-/-}$ mice causes cellular infiltration in liver, and transfer of *Tnfsf11*$^{-/-}$*Cd40*$^{-/-}$ splenocytes causes cellular infiltration in kidney (wild-type, n = 4; *Cd40*$^{-/-}$, n = 4; *Tnfsf11*$^{-/-}$, n = 4; *Tnfsf11*$^{-/-}$*Cd40*$^{-/-}$, n = 6; all mice are in a Balb/c background). Paraffin-embedded thymic sections were stained with hematoxylin and eosin (left panels: 40× magnification, scale bars represent 200 μm). Arrowheads indicate cellular infiltrations.

(B) Generation of autoantibodies in recipient mice transferred with *Tnfsf11*$^{-/-}$ and *Tnfsf11*$^{-/-}$*Cd40*$^{-/-}$ splenocytes. Sera of nude mice transferred with *Tnfsf11*$^{-/-}$*Cd40*$^{-/-}$, *Tnfsf11*$^{-/-}$, *Cd40*$^{-/-}$, or wild-type splenocytes were tested for the presence of autoantibodies (green) against liver and kidney from *Rag2*$^{-/-}$ mice. Nuclei are stained red with propidium iodide. Scale bars represent 200 μm.

DCs (Quezada et al., 2004; Theill et al., 2002), autoimmune reactions are suppressed in these mice. To circumvent such possible effects, we transferred splenocytes from *Tnfsf11*$^{-/-}$*CD40*$^{-/-}$, *Tnfsf11*$^{-/-}$, *CD40*$^{-/-}$, or control wild-type mice to athymic nude mice. When splenocytes from *Tnfsf11*$^{-/-}$*CD40*$^{-/-}$ mice were transferred, recipients' livers were shrunk (Figure S5A), suggesting severe liver injury in these recipients. Histological analyses of liver sections revealed severe cellular infiltrations when splenocytes from *Tnfsf11*$^{-/-}$ mice or *Tnfsf11*$^{-/-}$*Cd40*$^{-/-}$ mice were transferred (Figure 3A). On the other hand, recipients transferred with *Cd40*$^{-/-}$ mice or wild-type splenocytes were healthy and never showed cellular infiltration of any organs (Figure 3A). It should be noted that, when splenocytes of *Tnfsf11*$^{-/-}$*Cd40*$^{-/-}$ mice were transferred, cellular infiltration in the liver was more severe than when *Tnfsf11*$^{-/-}$ splenocytes were transferred (Figure 3A). In addition, transfer of *Tnfsf11*$^{-/-}$*Cd40*$^{-/-}$ splenocytes induced cellular infiltration around perivascular areas of recipients' kidneys (Figure 3A). Thus, the severity and organ specificity of cellular infiltration is correlated with the extent of mTEC defects.

To determine whether lymphocyte activation occurred in these recipient mice, we investigated generation of autoantibody against these organs by immunostaining frozen liver and kidney sections with sera obtained from these recipients. Serum from recipient nude mice transferred with *Tnfsf11*$^{-/-}$ or *Tnfsf11*$^{-/-}$*Cd40*$^{-/-}$ splenocytes contained autoantibody against liver cells. Recipients transferred with *Tnfsf11*$^{-/-}$*Cd40*$^{-/-}$ splenocytes had autoantibody against some kidney cells (Figure 3B). Thus, the generation of autoantibodies was quite consistent with cellular infiltration observed in the peripheral organs of recipients (compare Figure 3A and 3B). Although splenocytes transferred from deficient mice might lack tolerance for RANKL or CD40, the immunostaining observed with these sera was not attributable to antibodies against RANKL or CD40 because liver sections from *Tnfsf11*$^{-/-}$*Cd40*$^{-/-}$ (Figure S5B) or *Tnfsf11*$^{-/-}$ mice (data not shown) were also immunostained with these sera to the same extent as liver sections from wild-type mice. Overall, these data suggest that RANKL and CD40L signals are involved in inducing tolerance toward peripheral self-organs.

Ligation of RANK or CD40 Expressed in Thymic Stroma Leads to the Development of mTECs

In in vitro fetal thymic organ cultures, the interaction between hematopoietic cells and thymic stroma regulates development of mTECs. If the interaction between RANK expressed on thymic stroma and RANKL expressed in hematopoietic cells induces mTEC development, stimulation of 2-DG FTOC with recombinant RANKL might be sufficient to trigger the development of mature mTECs even in the absence of hematopoietic cells. To test this idea, we cultured 2-DG FTOC in the presence of recombinant RANKL for 4 days. Immunohistochemical analysis

revealed that mTECs expressing UEA-1-ligand, Cld3,4, and CD80 were induced in 2-DG FTOC in response to RANKL (Figure 4A). Flow-cytometric analysis confirmed the development of MHC class II$^+$UEA-1$^+$ mTECs by ligation of RANK during 2-DG FTOC (Figures 4B and 4C). The number of thymic stroma cells (gated on CD45-negative, TER119-negative cells) was also increased by RANKL ligation (Figure 4C). Consistent with the immunohistochemical analysis, the number of MHC class II$^+$UEA-1$^+$ mTECs was increased by approximately 50-fold at day 4 after RANKL administration. These data strongly suggested that RANKL triggers proliferation and differentiation of mTECs and/or their progenitors in 2-DG FTOC. The induction of mTEC markers was completely blocked by the addition of RANK-Fc chimeric protein, indicating that specific interaction between RANKL and RANK induces the development of mTECs. Quantitative and semiquantitative RT-PCR analyses indicated that the expression of Aire was induced by the ligation of RANK in 2-DG FTOC (Figure 4D and Figure S6). In addition, the expression of Aire-dependent and Aire-independent TSAs was significantly increased (Figure 4E and Figure S7). Immunohistochemical analysis showed the development of Aire-expressing cells upon stimulation with RANKL (Figure 4D), which is consistent with recent findings by others (Rossi et al., 2007). However, it should be noted that UEA-1$^+$Aire$^-$ cells did develop in RANKL-stimulated 2-DG FTOC. These data strongly suggested that RANKL-RANK interaction is sufficient for enabling development not only of Aire$^+$CD80$^+$ mTECs but also of Aire$^-$ mTECs expressing UEA-1-ligand, Cld3,4, and TSAs. Furthermore, together with the thymic phenotype of *Tnfsf11*$^{-/-}$ embryos, these data indicate that RANKL-RANK signaling in the embryonic thymus acts as a master switch to allow mTEC development.

Even if the fetal thymus does not express CD40L at early stages of embryogenesis, RT-PCR analysis revealed that CD40 is expressed from E13 (Figure S2). Given that CD40L signaling overlaps with RANKL stimulation, we speculated that the ligation of CD40 upon 2-DG FTOC would induce the development of mTECs. When 2-DG FTOC was cultured in the presence of recombinant CD40L for 4 days, UEA-1$^+$Aire$^+$ cells were indeed increased (Figure 5 and Figure S6). Quantitative and semiquantitative RT-PCR analysis further confirmed the increase in the expression of *Aire* and TSAs (Figure 5 and Figure S7). The induced development of mTECs expressing UEA-1 ligand, Aire, and TSAs was blocked by the addition of neutralizing CD40L antibody (Figure 5). Previous findings suggested that the LtβR signal is involved in the development of UEA-1-positive mTECs (Boehm et al., 2003; Venanzi et al., 2007) and expression of Aire (Chin et al., 2003). Therefore, we tested whether ligation of LtβR induces mTEC development and Aire expression in 2-DG FTOC. Immunohistochemical staining of 2-DG FTOC revealed practically no development of UEA-1$^+$ Aire$^+$ cells (Figure 5A). Quantitative RT-PCR analysis also indicated that ligation of LtβR is capable of inducing Aire expression, but its effect is considerably lower than that resulting from RANK or CD40 ligation (Figure 5B). These data suggest that stimulation with either RANK or CD40 is sufficient for the development of mTECs expressing Aire and Aire-dependent TSAs in 2-DG FTOC. Interestingly, ligation of LtβR induces the expression of *Crp*, which is an Aire-independent TSA (Figure 5C). This result is consistent with a recent report in which a reduced *Crp* expression was observed in the mTEC subset of *Ltβ*$^{-/-}$ mice (Seach et al., 2008). Overall, it is likely that RANK and CD40 signals are responsible for the development of the bulk of mature mTECs even if LtβR may be involved in development of a smaller TEC subset or in regulating a part of TSAs in mTECs.

Development of mTECs Induced by RANKL or CD40L Signal Requires TRAF6 and NIK

Previous studies suggested a requirement for both classical and nonclassical NF-κB activation pathways in the development of mTECs (Weih et al., 1995; Burkly et al., 1995; Zhang et al., 2007; Franzoso et al., 1997; Akiyama et al., 2005; Kajiura et al., 2004; Kinoshita et al., 2006). Because TRAF6 and NIK activate the classical and nonclassical NF-κB pathways, respectively, we investigated whether the development of mTECs induced by the ligation of RANK and CD40 requires TRAF6 and NIK as signal-transduction molecules. To address this issue, we prepared 2-DG FTOC from *Traf6*$^{-/-}$ or *aly/aly* embryos and stimulated them with recombinant RANKL or CD40L for 4 days. The development of UEA-1$^+$Aire$^+$ cells in response to ligation of RANK or CD40 was completely blocked in 2-DG FTOC of *Traf6*$^{-/-}$ and *aly/aly* mice (Figure 6A). In these experiments, the expression levels of RANK and CD40 in 2-DG FTOC were not significantly affected by the TRAF6 or functional NIK deficiencies (Figure S7). Furthermore, plausible progenitors of mTECs expressing claudine-3,4 appear to be present in these mutant mice (Figure S8), consistent with a previous obervation (Hamazaki et al., 2007). Quantitative and semiquantitative RT-PCR analysis further indicated that the expression of *Aire* and TSAs was also dependent on TRAF6 as well as NIK (Figures 6B and 6C and Figure S6). These data strongly suggest that ligation of RANK or CD40 leads to the activation of intracellular signaling pathways dependent on TRAF6 and NIK for the development of mTECs.

Because RelB is essential for the development of mTECs expressing UEA-1 ligand and Aire (Burkly et al., 1995; Weih et al., 1995; Zuklys et al., 2000), we investigated whether the ligation of RANK or CD40 induces the expression of RelB and its nuclear localization indicative of its activation. Immunohistochemical staining indicated that expression of RelB was increased by the ligation of RANK or CD40 in 2DG-FTOC (Figure 7A). Furthermore, RelB protein induced by RANK or CD40 ligation localized mainly to the nucleus (Figure 7A, arrows). This finding strongly suggested that the nonclassical NF-κB pathway is activated by RANK or CD40 signaling in mTECs. We previously suggested that a TRAF6-dependent signal activates the expression of RelB in mTEC cell lines (Akiyama et al., 2005), and that this might be a key step for the development of mTECs. Importantly, neither the expression nor the nuclear localization of RelB was observed when *Traf6*$^{-/-}$ or *aly/aly* 2-DG FTOC were stimulated with RANKL or CD40L (Figure 7A). Furthermore, the development of UEA-1$^+$Aire$^+$ mTECs induced by RANK ligation was inhibited in 2-DG FTOC prepared from *Relb*$^{-/-}$ embryonic thymus (Figure 7B). These data suggest that RANKL and CD40L signals activate TRAF6 and NIK to induce the expression and activation of RelB, which are essential for mTEC development.

The classical NF-κB activation pathway depends on a protein complex, called IKK complex, consisting of IKKα, IKKβ, and

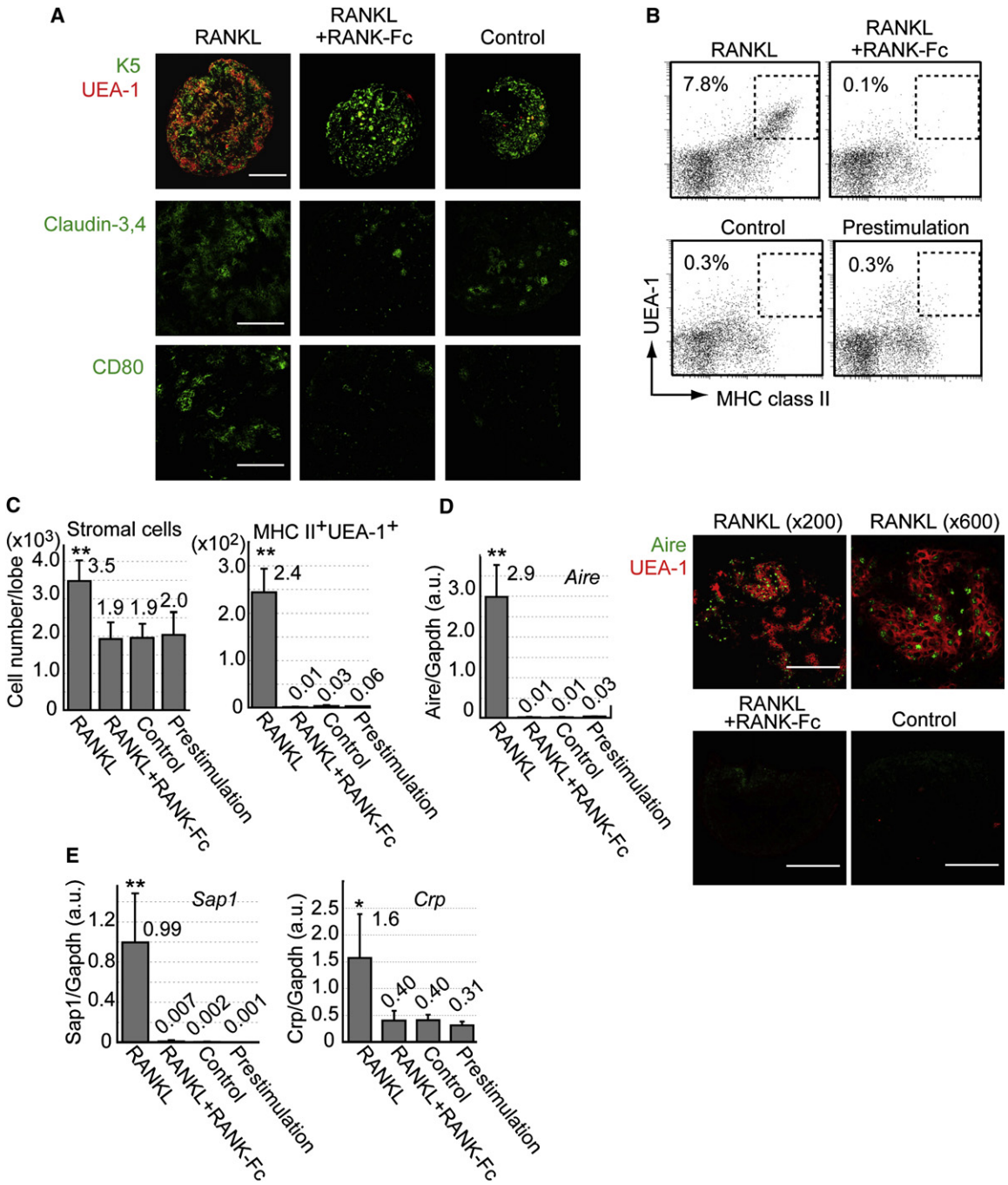

Figure 4. RANKL Signal Induces the Development of mTECs Expressing UEA-1 Ligand, MHC Class II, Cld3,4, CD80, Aire, and TSAs

(A) Immunostaining of 2-DG FTOC with a combination of anti-keratin-5 (green) and UEA-1 (red) (upper panels), anti-claudin-3 and -4 (green), or CD80 (lower panels) after stimulation with RANKL (left panels), with RANKL and RANK-Fc (middle panels), or without RANKL (right panels) for 4 days. Scale bars represent 200 μm for upper panels and 100 μm for middle and lower panels.

(B) Flow-cytometric analysis of 2-DG FTOC (prestimulation) and 2-DG FTOC stimulated by RANKL (RANKL), RANKL in the presence of RANK-Fc (RANKL-RANK-Fc), or RANKL in the absence of RANKL (sham) for 4 days. Cell suspensions from 12 to 16 thymic lobes were stained with UEA-1, anti-MHC class II (I-A/I-E), anti-CD45, and TER119 antibodies and analyzed by flow cytometry. The ratio of MHC class II$^+$, UEA-1$^+$ cells (in square) to thymic stromal cells (CD45, TER119 double-negative cells) is shown.

(C) Summary of the number of thymic stromal cells and mTECs induced by the ligation of RANK. Number of stromal cells (CD45$^-$, TER119$^-$) or UEA-1$^+$ MHC class II$^+$ mTECs per lobe was estimated from the results of the flow-cytometric analysis shown in Figure 4B. Error bars represent 1 SD above the mean (indicated above the bars) of at least three independent experiments.

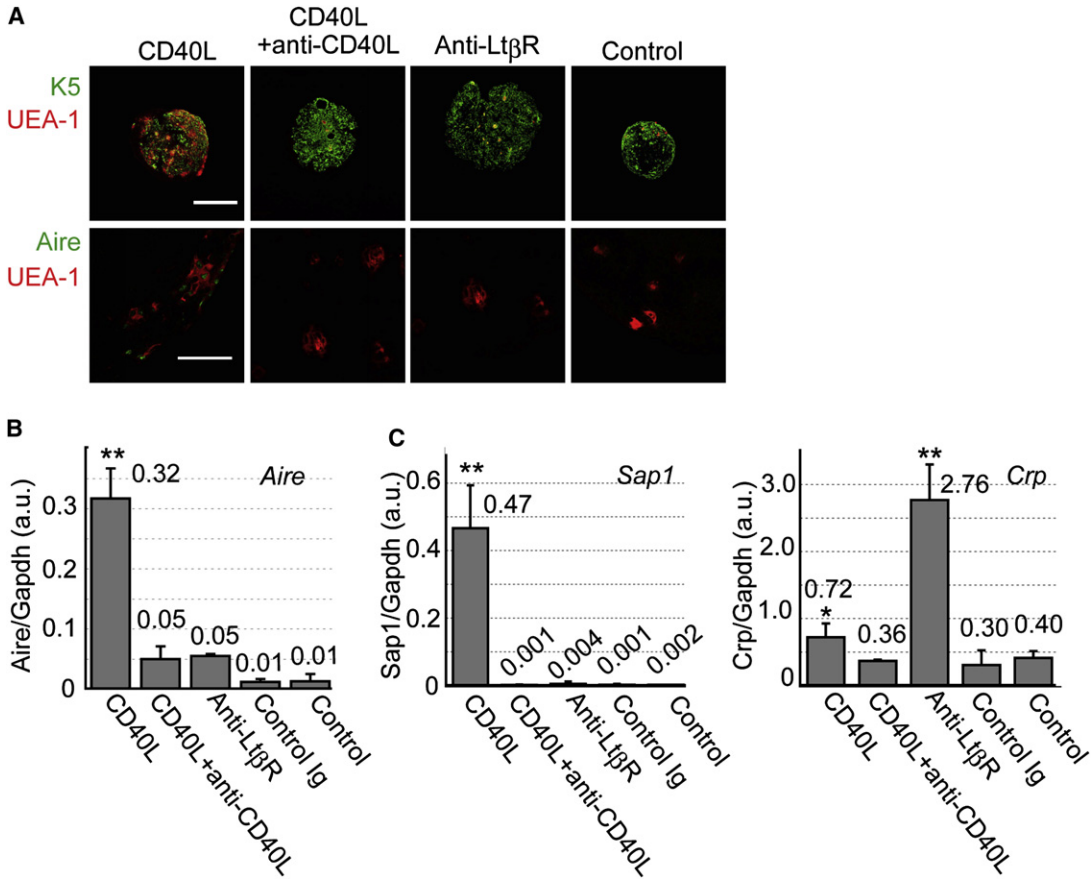

Figure 5. Ligation of CD40 Induces the Development of mTECs Expressing UEA-1-Ligand, Aire, and TSAs

(A) Immunostaining of 2-DG FTOC with a combination of keratin-5 antibody (green) and UEA-1 (red) (upper panels) or Aire antibody (green) and UEA-1 (red) (lower panels) after stimulation with CD40L, with CD40L and neutralizing anti-CD40L, with agonistic LtβR antibody, or without ligands for 4 days. Scale bars represent 200 μm for upper panels and 100 μm for lower panels.

(B) Real-time RT-PCR analyses of *Aire* transcript in 2-DG FTOC stimulated with CD40L, with CD40L and neutralizing anti-CD40L antibody, with agonistic LtβR antibody, with control antibody, or without ligand for 4 days (*$p < 0.05$ and **$p < 0.01$, Student's t test; n = 3). Values are arbitrary units normalized to *GAPDH*.

(C) Real-time RT-PCR analyses of TSA (*Sap1* and *Crp*) transcripts in 2-DG FTOC stimulated with CD40L, with CD40L and neutralizing anti-CD40L, with agonistic LtβR antibody, with control antibody, or without ligand for 4 days (*$p < 0.05$ and **$p < 0.01$, Student's t test; n = 3). Values are arbitrary units normalized to *GAPDH*. In (B) and (C), error bars represent 1 SD above the mean (indicated above the bars) of three independent experiments.

NEMO (IKKγ) (Bonizzi and Karin, 2004; Hoffmann and Baltimore, 2006). The phosphorylation of IκBα, which is an essential step for the nuclear localization of NF-κB, depends largely on IKKβ activity (Li et al., 1999a, 1999b). Because TRAF6 activates the classical NF-κB pathway, the requirement for TRAF6 in mTEC development suggested involvement of the classical NF-κB activation pathway induced by RANKL or CD40L. In order to verify this conjecture, SC-514, which specifically inhibits IKKβ activity by blocking its ATP binding site (Kishore et al., 2003), was added to the 2-DG FTOC stimulated with RANKL or CD40L. Importantly, the development of mTECs expressing Aire and TSAs was severely inhibited by the addition of SC-514 (Figures 7C and 7D and Figure S6). These data strongly suggest that activation of the classical NF-κB pathway is required for the development of mTECs induced by the ligation of RANK and CD40. Overall, our data show that the ligation of RANK or CD40 activates both classical and nonclassical NF-κB activation pathways to allow development of functional mTECs essential for self-tolerance.

DISCUSSION

In this study, we found that RANK and CD40 signals cooperatively regulate development of mTECs via NF-κB activation. Our study also indicates that in mTECs, signals from RANK as well as those from CD40 activate both classical and nonclassical

(D) Real-time RT-PCR analyses of *Aire*, TSA (*Sap1* and *Crp*) transcripts in 2-DG FTOC stimulated with RANKL, with RANKL and RANK-Fc, or without RANKL for 4 days (*$p < 0.05$ and **$p < 0.01$, Student's t test; n = 3). Values are arbitrary units normalized to *GAPDH*. Error bars represent 1 SD above the mean (indicated above the bars) of three independent experiments.

(E) Immunostaining of 2-DG FTOC with a combination of Aire antibody (green) and UEA-1 (red) after stimulation with RANKL, with RANKL and RANK-Fc, or without RANKL. The values in parentheses indicate the magnification. Scale bars represent 100 μm.

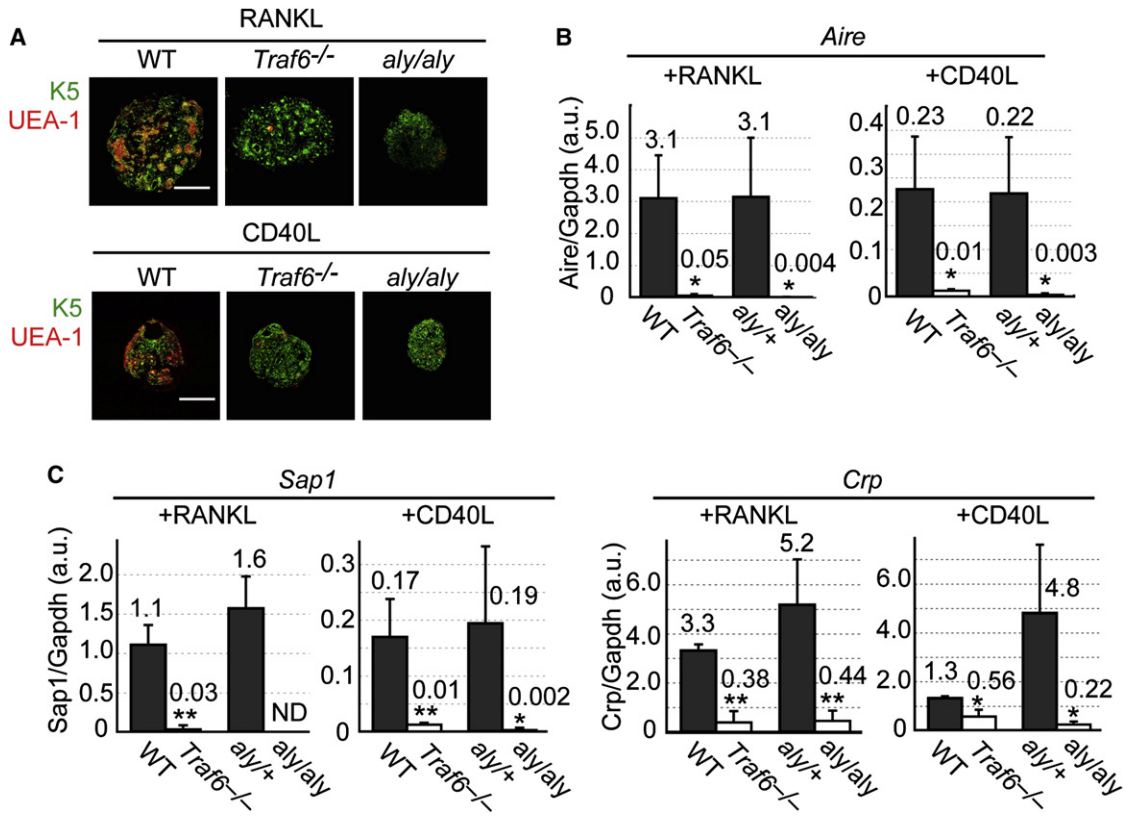

Figure 6. Development of mTECs Induced by Ligation of RANK and CD40 Depends on TRAF6 and Functional NIK

(A) Immunostaining of 2-DG FTOC from wild-type (left panels), *Traf6*$^{-/-}$ (middle panels), or *aly/aly* (right panels) with a combination of keratin-5 antibody (green) and UEA-1 (red) after stimulation with RANKL (upper panels) or CD40L (lower panels) for 4 days. Scale bars represent 200 μm.

(B) Real-time RT-PCR analyses of *Aire* transcript in 2-DG FTOC from wild-type mice or *Traf6*$^{-/-}$ stimulated with CD40L, with CD40L and neutralizing anti-CD40L, with agonistic LtβR antibody, with control antibody, or without ligand for 4 days (*$p < 0.05$ and **$p < 0.01$, Student's t test; n = 3). Values are arbitrary units normalized to *GAPDH*.

(C) Real-time RT-PCR analyses of TSA (*Sap1* and *Crp*) transcripts in 2-DG FTOC from wild-type mice or *Traf6*$^{-/-}$ stimulated with CD40L, with CD40L and neutralizing anti-CD40L, or without ligand for 4 days (*$p < 0.05$ and **$p < 0.01$, Student's t test; n = 3). Values are arbitrary units normalized to *GAPDH*. In (B) and (C), error bars represent 1 SD above the mean (indicated above the bars) of three independent experiments.

NF-κB pathways, in turn inducing transcriptional activation of RelA-p50 and RelB-p52 complexes, respectively. It has been reported that the expression of RelB is regulated by transcriptional activation of RelA (Bren et al., 2001), which is downstream of the classical NF-κB pathway. Therefore, it is most likely that the classical NF-κB pathway activated by RANK or CD40 would induce the expression of RelB and that the nonclassical pathway is subsequently activated to induce the translocation of RelB into the nucleus. Interestingly, we found that NIK as well as TRAF6 is essential for the expression of RelB in mTECs in vitro. In many types of cells, NIK induces phophorylation of IKKα complex, which in turn activates the nonclassical NF-κB pathway (Hoffmann and Baltimore, 2006; Bonizzi and Karin, 2004). However, our data suggested that NIK may somehow be involved in the classical NF-κB activation pathway with respect to the expression of RelB. There are two possible explanations for these observations. The first is that NIK may be downstream of TRAF6, and that it activates the classical NF-κB activation pathway in mTECs. It has been reported that NIK deficiency in lymphoblastoid cells causes a defect in both the classical and nonclassical NF-κB activation pathways induced by the ligation of CD40 (Ramakrishnan et al., 2004), suggesting that NIK is involved in the activation of the classical NF-κB pathway induced by TNFRSF. Although NIK is apparently not required for the activation of the classical NF-κB pathway in bone-marrow-derived macrophages (Novack et al., 2003), it is still possible that the requirement for NIK in the classical pathway induced by RANK or CD40 is dependent on cell type. The other possibility is that NIK does not directly activate the classical NF-κB pathway but enhances the transcriptional activity of RelA. For instance, it has been reported that NIK induces phosphorylation of histone H3 via IKKα (Park et al., 2006). Histone H3 phosphorylation enhances NF-κB-directed gene expression (Anest et al., 2003; Yamamoto et al., 2003). Interestingly, recent studies suggested that RANK signals induce the nuclear localization of phospho-IKKα (Luo et al., 2007). Therefore, it is possible that RANK signaling activates NIK to induce phosphorylation and nuclear localization of IKKα. The phosphorylated IKKα, in turn, might enhance the transcriptional activity of RelA for the expression of RelB.

Relb$^{-/-}$ mice are known to be severely defective in the development of mature mTECs expressing Aire (Burkly et al., 1995; Heino et al., 2000; Weih et al., 1995). Because both RANK and

CD40 signals were reported to activate the noncanonical NF-κB activation pathway (Bonizzi and Karin, 2004; Hoffmann and Baltimore, 2006; Novack et al., 2003), our finding of severe defects in mTEC development in *Tnfsf11*$^{-/-}$*Cd40*$^{-/-}$ mice is consistent with the idea that the nonclassical NF-κB pathway is essential for the development of mTECs. Two independent groups reported that NF-κB2, which binds to RelB in the nonclassical pathway, is involved in the expression of Aire and TSAs or other mTEC markers (Zhang et al., 2007; Zhu et al., 2006). However, it should be noted that the disruption of thymic medullar architecture of *Nfκb2*$^{-/-}$ mice is mild (Zhang et al., 2007; Zhu et al., 2006). The inconsistency in the thymic phenotype between *Relb*$^{-/-}$ and *Nfkb2*$^{-/-}$ mice may be explained by the idea that the nonclassical NF-κB pathway is involved in two distinct and consecutive processes, the first being the development of mature mTECs and the second the expression of Aire and TSAs, and these two processes may have different dependency on NF-κB2. Thus, the requirement for NF-κB2 in the first process may be substituted for by NF-κB1, which also binds to RelB (Hoffmann and Baltimore, 2006). However, NF-κB1 may only partially substitute for NF-κB2 in the second process. This idea is consistent with the observation that NF-κB1 and NF-κB2 doubly deficient mice showed defects in thymic architecture as severe as *Relb*$^{-/-}$ or *Tnfsf11*$^{-/-}$*Cd40*$^{-/-}$ mice (Franzoso et al., 1997).

Anderson's group reported that lymphoid tissue inducer (Lti) cells express RANKL, thereby promoting the development of mTECs for self-tolerance (Rossi et al., 2007). They also found that ligation of RANK in thymic stroma induces Aire and CD80 expression (Rossi et al., 2007). In this study, we found that RANKL ligation induces not only Aire and Aire-dependent TSAs, but also UEA-1 ligand, Cld3, 4, and Aire-independent TSAs. Notably, our immunohistochemical study revealed that RANKL induces UEA-1^{+}Aire^{-} mTECs in addition to UEA^{+}Aire^{+} mTECs. Furthermore, our in vivo study suggests that RANKL-RANK and CD40L-CD40 signals cooperate to regulate the medullar organization and development of both Aire^{+} and Aire^{-} mTECs. Therefore, the function of RANK is not restricted in the development of Aire-expressing mTECs but also regulates Aire-negative mTECs, as would be required for organization of the thymic medullar architecture in postnatal mice. For developing or maintaining mTECs, expression of RANKL should be maintained from embryo through to adulthood. Other cells in addition to Lti cells may be required as a source of RANKL expression, because the ratio of Lt*i* in adult thymus is considerably lower. Hikosaka et al. (2008) found that expression of both RANKL and CD40L on thymocytes was increased in cells undergoing positive selection. This result suggests that RANKL produced by single-positive T cells in addition to Lt*i* is required for the differentiation, proliferation, and/or maintenance of mTECs in adult mice.

We also found that RANKL signaling acts as a master switch to induce TSAs in the embryonic thymus. It has been reported that expression of TSAs appears to be epigenetically regulated (Kyewski and Klein, 2006). Therefore, RANKL might stimulate epigenetic changes in mTEC progenitors and then induce TSAs. At present, two models have been proposed to explain the diverse expression patterns of TSAs in mTECs. The "terminal differentiation model" proposes that expression of TSAs becomes increasingly diverse during the maturation from progenitor cells to MHC class II^{lo}, CD80^{lo} mTECs and MHC classII^{hi}, CD80^{hi} mTECs (Kyewski and Klein, 2006). The "developmental restriction model" proposes that immature mTECs each express a diverse battery of genes, and that differentiation of mTECs progressively restricts the diversity of TSAs (Farr et al., 2002). In the "terminal differentiation model," RANKL signaling induces the initial differentiation of mTECs and expression of TSAs commences subsequently. In contrast, in the "developmental restriction model," RANKL would induce the expression of TSAs in the TEC progenitors, thereby triggering the differentiation process. Future studies on the expression kinetics of TSAs induced by ligation of RANK upon 2-DG FTOC should clarify which of these two models is the more appropriate.

It has previously been proposed that RANKL-RANK and CD40L-CD40 signals have fundamentally different functions in the control of immune responses and organ development (Theill et al., 2002). Expression of both CD40L and RANKL is upregulated on activated T cells, and both CD40 and RANK are expressed on DCs (Theill et al., 2002) (Walsh and Choi, 2003). However, in contrast to the CD40L-CD40 signal, RANKL-RANK signal did not affect the expression of DC activation markers but instead enhanced DC survival by inducing Bcl-xL (Wong et al., 1997). In this study, we found that both RANKL and CD40L signals induce the development of mTECs. RANKL signal was essential and sufficient for the development of mTECs in embryos. The contributions of CD40L signaling to mTEC development started in neonatal mice. Thus, after birth, cooperation between the RANKL and CD40L signals appears to be required for establishing intact medullary development in postnatal mice. This finding implies that, in addition to mTEC development, RANK and CD40 signals may also cooperate in other immune responses or aspects of organogenesis.

The data that either RANKL or CD40L is sufficient for inducing mature mTEC development along with the expression of Aire and TSAs in 2-DG FTOC suggests a redundancy of two signals in mTEC development. However, the redundancy of RANK and CD40 signals should be only partial, and synergy between the two signals is required for development of intact thymic architecture; RANKL or CD40 singly deficient mice are partially defective in mTEC development. In addition, our quantitative RT-PCR analysis and comparison of mTEC development between *Tnfsf11*$^{-/-}$ and *CD40*$^{-/-}$ mice suggests that the RANK signal plays a dominant role in mTEC development or proliferation. Importantly, flow-cytometric analysis suggested that RANKL preferentially regulates the development of the MHC class II^{hi} subset of mTECs, and CD40L is rather preferentially involved in development of MHC class II^{lo} mTECs. Therefore, RANK and CD40 signals should have partially distinct functions in mTEC development. Interestingly, ligation of LtβR induces Aire expression at very low levels in 2-DG FTOC but efficiently induces *Crp*, which is an *Aire*-independent TSA. These data are consistent with a recent report by Boyd and coworkers, in which the expression of *Crp* was severely reduced in *Lt*$\alpha^{-/-}$ and *Lt*$\beta^{-/-}$ mice (Seach et al., 2008). The differences in function among these ligands demand future clarification.

It was previously shown that Aire controls negative selection of organ-specific T cells (Liston et al., 2003). We and others have found that RANKL-RANK signal is involved in the development of mTECs expressing Aire (Rossi et al., 2007; Hikosaka et al., 2008). These data suggest that RANKL-RANK interaction

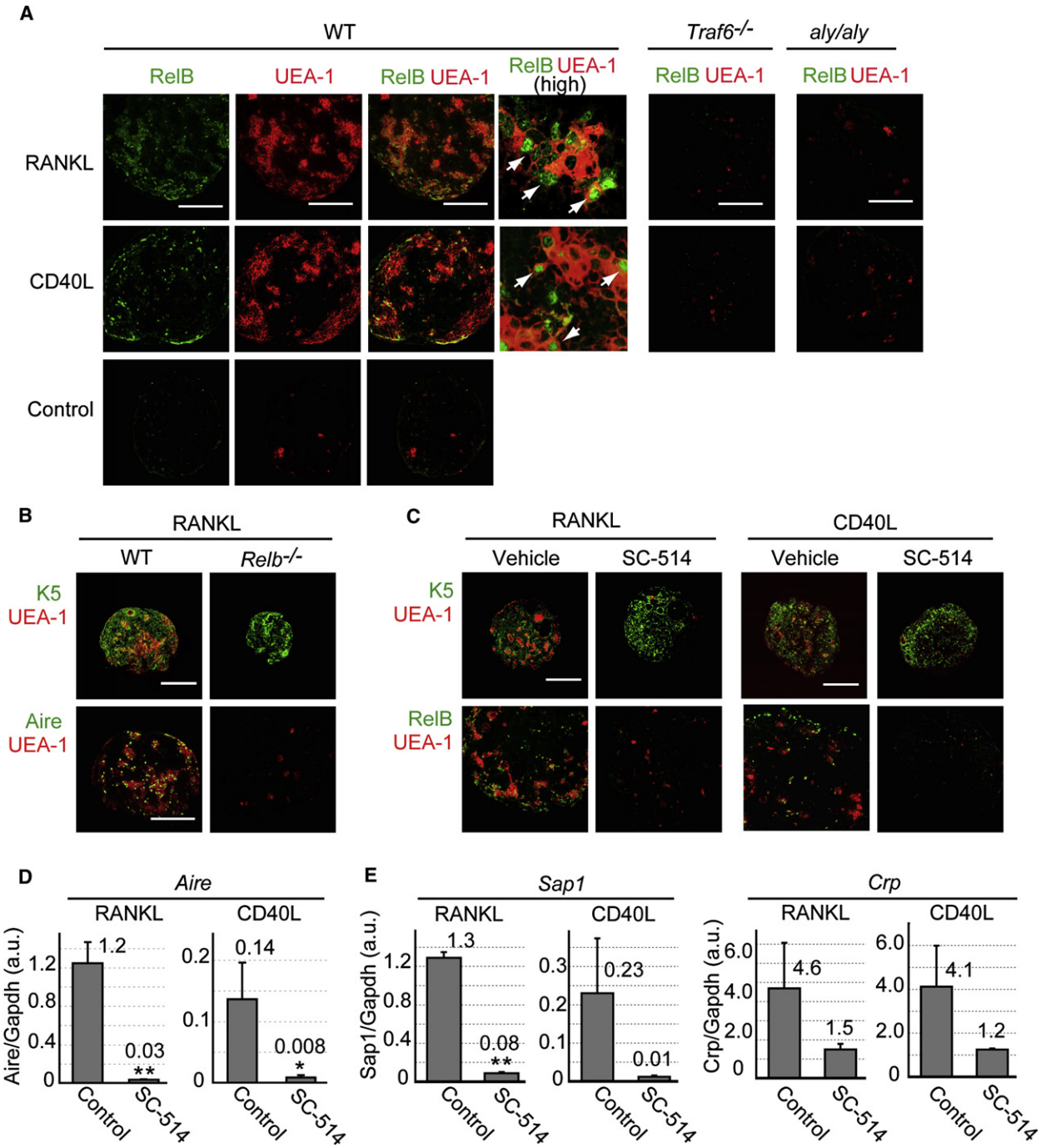

Figure 7. Ligation of RANK and CD40 Induces TRAF6-, NIK-, and IKKβ-Dependent Activation of NF-κB in 2-DG FTOC

(A) Ligation of RANK and CD40 induces the expression and nuclear localization of RelB dependent on TRAF6 and NIK. Immunostaining of 2-DG FTOC from wild-type, *Traf6*$^{-/-}$, or *aly/aly* with a combination of RelB antibody (green) and UEA-1 (red) after stimulation with RANKL (upper panels), with CD40L (middle panels), or without ligand (lower panels) for 4 days. Scale bars represent 200 μm. Panels labeled "RelB UEA-1" show merged images of RelB and UEA-1 staining. Panels labeled "RelB UEA-1 (High)" show highly magnified images of RelB and UEA-1 merged images. Arrows in the panels indicate typical examples of nuclear-localized RelB staining (green).

(B) Development of mTECs expressing UEA-1 and Aire induced by RANK ligation is dependent on RelB. Immunostaining of 2-DG FTOC from wild-type, or *Relb*$^{-/-}$ with a combination of keratin-5 antibody (green) and UEA-1(red) (upper panels), or a combination of Aire antibody (green) and UEA-1 (red) after stimulation with RANKL (upper panels) for 4 days.

(C) Development of mTECs induced by ligation of RANK and CD40 is inhibited by an IKKβ-specific inhibitor. Immunostaining of 2-DG FTOC from wild-type with a combination of keratin-5 antibody (green) and UEA-1 (red) (upper panels), or a combination of RelB antibody (green) and UEA-1(red) (lower panels), after stimulation with RANKL or CD40L in the presence of SC-514 or an equal volume of its solvent for 4 days.

regulates negative selection of self-reactive T cells by promoting the development of Aire-positive mTECs. Consistent with this hypothesis, it was reported that transplantation of *Rank*$^{-/-}$ thymic stroma sufficed to induce autoimmunity in athymic nude mice (Rossi et al., 2007), suggesting the requirement of RANK signaling in mTECs for negative selection. We also found that the transfer of splenocytes from *Tnfsf11*$^{-/-}$ mice into nude mice results in cellular infiltrations and generation of organ-specific antibodies. This result, together with the previous findings in *Rank*$^{-/-}$ mice, reveals a critical role of RANKL-RANK interaction in establishing self-tolerance.

Defects of the development of mTECs expressing Aire and TSAs in *Tnfsf11*$^{-/-}$*Cd40*$^{-/-}$ thymus were more severe than those in single *Tnfsf11*$^{-/-}$ or *Cd40*$^{-/-}$ mice. These data imply that negative selection by mTECs expressing Aire and TSAs is more severely impaired in *Tnfsf11*$^{-/-}$*Cd40*$^{-/-}$ thymus than in *Tnfsf11*$^{-/-}$ or *Cd40*$^{-/-}$ thymus, which may generate a more diverse set of self-reactive T cells in *Tnfsf11*$^{-/-}$*Cd40*$^{-/-}$ mice than in *Tnfsf11*$^{-/-}$ or *Cd40*$^{-/-}$ mice. In fact, autoimmune phenotypes in recipients of *Tnfsf11*$^{-/-}$*Cd40*$^{-/-}$ splenocytes were remarkably more severe than recipients of *Tnfsf11*$^{-/-}$ splenocytes, and recipients of *Cd40*$^{-/-}$ splenocytes did not develop autoimmunity. Importantly, the severity of autoimmunity is positively correlated with impairment of mTEC development among these mice, in agreement with the idea that autoimmunity observed in these recipients can be ascribed to the mTEC defects of the donors.

Even if no sign of autoimmunity in *Cd40*$^{-/-}$ mice was observed at 2 weeks after birth, deficiency in CD40 appears to greatly exacerbate autoimmunity in *Tnfsf11*$^{-/-}$ mice. Furthermore, cellular infiltration in kidney and generation of antibodies specific to kidney cells were detected only in recipients of *Tnfsf11*$^{-/-}$*Cd40*$^{-/-}$ splenocytes, and not in those that received *Tnfsf11*$^{-/-}$ splenocytes. These findings suggest the involvement of CD40 signaling in self-tolerance. Notably, we found partly overlapping functions for CD40 and RANK signals in inducing the development of Aire- and TSA-positive mTECs in vitro and in vivo. Thus, our data suggest that RANK and CD40 signals cooperatively establish an intact thymic environment to regulate the negative selection of organ-specific T cells.

In summary, we determined that RANKL and CD40L are key cytokine signals for the development of mTECs in a TRAF6- and NIK-dependent manner. More detailed analyses of self-tolerance in these mutant mice should be carried out to clarify the molecular mechanism by which these cytokines control the thymic environment and immune disease. Such information will be beneficial in developing therapeutic strategies for the treatment of immune-system disorders.

EXPERIMENTAL PROCEDURES

Mice

Tnfsf11$^{-/-}$, *Cd40*$^{-/-}$, and *Traf6*$^{-/-}$ have been described previously (Akiyama et al., 2005; Kawabe et al., 1994; Kong et al., 1999). These mice were backcrossed onto Balb/c or C57BL/6 mice at least seven times. Thymic phenotypes were independent of genetic backgrounds of mice. *Relb*$^{-/-}$ mice were purchased from the Jackson Laboratory, and *aly/aly* and *aly*/+ mice were purchased from CLEA, Japan. All the mice were maintained under specific-pathogen-free conditions and were handled in accordance with the Guidelines for Animal Experiments of the Institute of Medical Science, University of Tokyo (Japan). The morning of finding a vaginal plug was designated as embryonic day 0 (E0).

Antibodies and Reagents

Rabbit anti-mouse keratin-5 was purchased from Covance (Berkeley, CA). Biotinylated UEA-1 was obtained from VECTOR Laboratories (Burlingame, CA). Rabbit anti-mouse Aire was described (Kajiura et al., 2004). Phycoerythrin (PE)-conjugated rat anti-mouse CD8a (Ly2) and rat anti-mouse Ep-CAM were obtained from BD PharMingen. Rat anti-mouse CD80, PE-conjugated rat anti-CD45, PE-conjugated mouse TER-119, and FITC-conjugated mouse MHC class II (M5/114.15.1) were obtained from eBioscience. Rabbit anti-claudin-3 and claudin-4 were obtained from ZYMED Laboratories (South San Francisco, CA). ER-TR5 was kindly gifted from M. Itoi. Recombinant mouse RANKL was obtained from WAKO (Tokyo, Japan). Rabbit anti-mouse RelB (sc-226) was obtained from Santa Cruz. Recombinant mouse CD40 and goat anti-mouse CD40 ligand were obtained from R&D Systems. RANK-Fc chimera was obtained from SIGMA. Secondary reagents, Alexa fluor 488-conjugated goat anti-rabbit IgG, Alexa fluor 546-conjugated streptavidin, Alexa fluor 488-conjugated anti-rat IgG, and Alexa fluor 546-conjugated anti-rat IgG were obtained from Invitrogen (Carlsbad, CA). SC-514 was obtained from CALBIOCHEM.

Fetal Thymus Organ Culture, FTOC

Thymic lobes were isolated from embryos 14 days after coitus and were cultured for 4 days on Nucleopore filters (Whatmann, Clifton, NJ) placed in R10 medium containing RPMI1640 (Invitrogen), supplemented with 10% fetal bovine serum (FBS) (Equitech-Bio, Kerrville, TX), 2 mM L-glutamine (Wako Chemicals, Osaka, Japan), 100 U/ml penicillin (Banyu Pharmaceutical, Tokyo, Japan), 100 μg/ml streptomycin (Meiji Seika Kaisha, Tokyo, Japan), and 50 μM 2-mercaptoethanol (Wako) containing 1.35 mM 2′-deoxyguanosine (2-DG) (Sigma-Aldrich, St. Louis, MO). Fetal thymic stroma (2-DG FTOC) was cultured in R10 with recombinant RANKL (1 μg/ml) or CD40L (5 μg/ml). For the blocking experiments, RANK-Fc chimera (5 μg/ml), anti-CD40L (10 μg/ml), or SC-514 (100 μM) was added in the medium. Four days after the ligation, the 2-DG FTOC was recovered and used for the analyses.

Histopathology and Immunohistochemistry

Tissues were immersion-fixed in 10% buffered formalin (Wako) and embedded in paraffin blocks. Sections (4 μm thick) were stained with hematoxylin-eosin and examined by light microscopy. For immunohistochemistry, tissues were embedded in OCT compound (Sakura Finetech, Tokyo, Japan) and frozen in liquid nitrogen. Cryostat sections (6 μm thick) were fixed by immersion for 10 min in ice-cold acetone and incubated with primary antibody for 1 hr at room temperature. Sections were washed with phosphate-buffered saline (PBS) and then incubated with secondary antibody for 40 min at room temperature. Confocal color images were obtained with a Radiance 2000 confocal microscope (Bio-Rad Laboratories).

Semiquantitative RT-PCR

RNA was extracted from whole thymus or 2-DG FTOC with either an RNeasy Mini or Micro Kit (QIAGEN). Total RNA was subjected to random-primed reverse transcription with a cDNA cycle kit (Invitrogen). Primer sets for PCR and amplification conditions have been described previously (Akiyama et al., 2005). For real-time PCR analysis of Aire and GAPDH, TaqMan

(D) Expression of *Aire* induced by the ligation of RANK or CD40 was inhibited by an IKKβ-specific inhibitor. Real-time RT-PCR analyses of *Aire* transcript in 2-DG FTOC from wild-type mice stimulated with RANKL or CD40L in the presence of SC-514 or its solvent for 4 days (*$p < 0.05$ and **$p < 0.01$, Student's t test; n = 3). Values are arbitrary units normalized to *GAPDH*. Error bars represent 1 SD above the mean (indicated above the bars) of three independent experiments.
(E) Expression of TSAs induced by the ligation of RANK or CD40 was inhibited by an IKKβ-specific inhibitor. Real-time RT-PCR analyses of *Sap1* and *Crp* transcripts in 2-DG FTOC from wild-type mice stimulated with RANKL or CD40L in the presence of SC-514 or its solvent for 4 days (*$p < 0.05$ and **$p < 0.01$, Student's t test; n = 3). Values are arbitrary units normalized to *GAPDH*.

gene-expression assay (ABI) was carried out according to the manufacturer's protocol. For the quantitative analysis, we specifically used mice at postnatal day (PN) 14 to 16.

Flow-Cytometric Analysis

Single-cell suspensions from whole thymus were prepared by digesting in RPMI 1640 medium containing collagenase/disperse (Roche) and DNase I (Takara). Dead cells were excluded from the analysis by means of 7-aminoactinomycin D (Wako) staining. Stained cells were analyzed with a fluorescence-activated cell sorter (Epics XL; Beckmann Coulter, Fullerton, CA).

Splenocyte Transfer

Splenocytes were prepared from mutant and control mice (wild-type, n = 4; *Cd40*$^{-/-}$, n = 4; *Tnfsf11*$^{-/-}$, n = 4; *Tnfsf11*$^{-/-}$*Cd40*$^{-/-}$, n = 6; all mice are of a Balb/c background). Before injection, splenocytes were analyzed by flow cytometry, and the number of T cells injected in mice was adjusted. Splenocytes are intravenously injected into Balb/c nude mice and analyzed 6 weeks after the injection. Histochemical analysis and immunostaining of liver and kidney sections with sera were described.

Statistical Analysis

p values were calculated with the Student's t test with Microsoft Excel software, with two-tailed distribution and two-sample unequal variance parameters.

SUPPLEMENTAL DATA

Supplemental Data include eight figures and can be found with this article online at http://www.immunity.com/cgi/content/full/29/3/423/DC1/.

ACKNOWLEDGMENTS

This work was supported by a grand-in-aid for scientific research from the Precursory Research for Embryonic Science and Technology (PRESTO) program of the Japan Science and Technology Agency (T.A.); a grant from the Japanese Society for the Promotion of Science (T.A.); grants for Priority Area Research from the Ministry of Education, Culture, Sports, Science and Technology of Japan (T.A. and J.I.); and a grant for the Genome Network Project from the Ministry of Education, Culture, Sports, Science and Technology of Japan (J.I.). J.M.P. is supported by Institute of Molecular Biotechnology of the Austrian Academy Sciences and by a grant by the European Commission, EURO-THYMAIDE. The authors thank R. Whittier for critical reading of the manuscript and other laboratory members for technical help and useful discussion.

Received: December 7, 2007
Revised: April 9, 2008
Accepted: June 20, 2008
Published online: September 18, 2008

REFERENCES

Aaltonen, J., and Bjorses, P. (1999). Cloning of the APECED gene provides new insight into human autoimmunity. Ann. Med. *31*, 111–116.

Akiyama, T., Maeda, S., Yamane, S., Ogino, K., Kasai, M., Kajiura, F., Matsumoto, M., and Inoue, J. (2005). Dependence of self-tolerance on TRAF6-directed development of thymic stroma. Science *308*, 248–251.

Anderson, M.S., Venanzi, E.S., Klein, L., Chen, Z., Berzins, S.P., Turley, S.J., von Boehmer, H., Bronson, R., Dierich, A., Benoist, C., and Mathis, D. (2002). Projection of an immunological self shadow within the thymus by the aire protein. Science *298*, 1395–1401.

Anderson, G., Lane, P.J., and Jenkinson, E.J. (2007). Generating intrathymic microenvironments to establish T-cell tolerance. Nat. Rev. Immunol. *7*, 954–963.

Anest, V., Hanson, J.L., Cogswell, P.C., Steinbrecher, K.A., Strahl, B.D., and Baldwin, A.S. (2003). A nucleosomal function for IkappaB kinase-alpha in NF-kappaB-dependent gene expression. Nature *423*, 659–663.

Boehm, T., Scheu, S., Pfeffer, K., and Bleul, C.C. (2003). Thymic medullary epithelial cell differentiation, thymocyte emigration, and the control of autoimmunity require lympho-epithelial cross talk via LTbetaR. J. Exp. Med. *198*, 757–769.

Bonizzi, G., and Karin, M. (2004). The two NF-kappaB activation pathways and their role in innate and adaptive immunity. Trends Immunol. *25*, 280–288.

Bren, G.D., Solan, N.J., Miyoshi, H., Pennington, K.N., Pobst, L.J., and Paya, C.V. (2001). Transcription of the RelB gene is regulated by NF-kappaB. Oncogene *20*, 7722–7733.

Burkly, L., Hession, C., Ogata, L., Reilly, C., Marconi, L.A., Olson, D., Tizard, R., Cate, R., and Lo, D. (1995). Expression of relB is required for the development of thymic medulla and dendritic cells. Nature *373*, 531–536.

Chin, R.K., Lo, J.C., Kim, O., Blink, S.E., Christiansen, P.A., Peterson, P., Wang, Y., Ware, C., and Fu, Y.X. (2003). Lymphotoxin pathway directs thymic Aire expression. Nat. Immunol. *4*, 1121–1127.

Clegg, C.H., Rulffes, J.T., Haugen, H.S., Hoggatt, I.H., Aruffo, A., Durham, S.K., Farr, A.G., and Hollenbaugh, D. (1997). Thymus dysfunction and chronic inflammatory disease in gp39 transgenic mice. Int. Immunol. *9*, 1111–1122.

Derbinski, J., Schulte, A., Kyewski, B., and Klein, L. (2001). Promiscuous gene expression in medullary thymic epithelial cells mirrors the peripheral self. Nat. Immunol. *2*, 1032–1039.

Dunn, R.J., Luedecker, C.J., Haugen, H.S., Clegg, C.H., and Farr, A.G. (1997). Thymic overexpression of CD40 ligand disrupts normal thymic epithelial organization. J. Histochem. Cytochem. *45*, 129–141.

Farr, A.G., Dooley, J.L., and Erickson, M. (2002). Organization of thymic medullary epithelial heterogeneity: Implications for mechanisms of epithelial differentiation. Immunol. Rev. *189*, 20–27.

Franzoso, G., Carlson, L., Xing, L., Poljak, L., Shores, E.W., Brown, K.D., Leonardi, A., Tran, T., Boyce, B.F., and Siebenlist, U. (1997). Requirement for NF-kappaB in osteoclast and B-cell development. Genes Dev. *11*, 3482–3496.

Gray, D.H., Seach, N., Ueno, T., Milton, M.K., Liston, A., Lew, A.M., Goodnow, C.C., and Boyd, R.L. (2006). Developmental kinetics, turnover, and stimulatory capacity of thymic epithelial cells. Blood *108*, 3777–3785.

Hamazaki, Y., Fujita, H., Kobayashi, T., Choi, Y., Scott, H.S., Matsumoto, M., and Minato, N. (2007). Medullary thymic epithelial cells expressing Aire represent a unique lineage derived from cells expressing claudin. Nat. Immunol. *8*, 304–311.

Heino, M., Peterson, P., Sillanpaa, N., Guerin, S., Wu, L., Anderson, G., Scott, H.S., Antonarakis, S.E., Kudoh, J., Shimizu, N., et al. (2000). RNA and protein expression of the murine autoimmune regulator gene (Aire) in normal, RelB-deficient and in NOD mouse. Eur. J. Immunol. *30*, 1884–1893.

Hikosaka, Y., Nitta, T., Ohigashi, I., Yano, K., Ishimaru, N., Hayashi, Y., Matsumoro, M., Matsuo, K., Penninger, J.M., Takayanagi, H., et al. (2008). The cytokine RANKL produced by positively selected thymocytes fosters medullary thymic epithelial cells that express autoimmune regulator. Immunity *29*, this issue, 438–450.

Hoffmann, A., and Baltimore, D. (2006). Circuitry of nuclear factor kappaB signaling. Immunol. Rev. *210*, 171–186.

Inoue, J., Gohda, J., and Akiyama, T. (2007). Characteristics and biological functions of TRAF6. Adv. Exp. Med. Biol. *597*, 72–79.

Ishida, T., Mizushima, S., Azuma, S., Kobayashi, N., Tojo, T., Suzuki, K., Aizawa, S., Watanabe, T., Mosialos, G., Kieff, E., et al. (1996). Identification of TRAF6, a novel tumor necrosis factor receptor-associated factor protein that mediates signaling from an amino-terminal domain of the CD40 cytoplasmic region. J. Biol. Chem. *271*, 28745–28748.

Kajiura, F., Sun, S., Nomura, T., Izumi, K., Ueno, T., Bando, Y., Kuroda, N., Han, H., Li, Y., Matsushima, A., et al. (2004). NF-kappa B-inducing kinase establishes self-tolerance in a thymic stroma-dependent manner. J. Immunol. *172*, 2067–2075.

Kawabe, T., Naka, T., Yoshida, K., Tanaka, T., Fujiwara, H., Suematsu, S., Yoshida, N., Kishimoto, T., and Kikutani, H. (1994). The immune responses in CD40-deficient mice: Impaired immunoglobulin class switching and germinal center formation. Immunity *1*, 167–178.

Kinoshita, D., Hirota, F., Kaisho, T., Kasai, M., Izumi, K., Bando, Y., Mouri, Y., Matsushima, A., Niki, S., Han, H., et al. (2006). Essential role of IkappaB kinase alpha in thymic organogenesis required for the establishment of self-tolerance. J. Immunol. *176*, 3995–4002.

Kishore, N., Sommers, C., Mathialagan, S., Guzova, J., Yao, M., Hauser, S., Huynh, K., Bonar, S., Mielke, C., Albee, L., et al. (2003). A selective IKK-2 inhibitor blocks NF-kappa B-dependent gene expression in interleukin-1 beta-stimulated synovial fibroblasts. J. Biol. Chem. *278*, 32861–32871.

Kobayashi, N., Kadono, Y., Naito, A., Matsumoto, K., Yamamoto, T., Tanaka, S., and Inoue, J. (2001). Segregation of TRAF6-mediated signaling pathways clarifies its role in osteoclastogenesis. EMBO J. *20*, 1271–1280.

Kobayashi, T., Walsh, M.C., and Choi, Y. (2004). The role of TRAF6 in signal transduction and the immune response. Microbes Infect. *6*, 1333–1338.

Kong, Y.Y., Yoshida, H., Sarosi, I., Tan, H.L., Timms, E., Capparelli, C., Morony, S., Oliveira-dos-Santos, A.J., Van, G., Itie, A., et al. (1999). OPGL is a key regulator of osteoclastogenesis, lymphocyte development and lymph-node organogenesis. Nature *397*, 315–323.

Kyewski, B., and Klein, L. (2006). A central role for central tolerance. Annu. Rev. Immunol. *24*, 571–606.

Li, Z.W., Chu, W., Hu, Y., Delhase, M., Deerinck, T., Ellisman, M., Johnson, R., and Karin, M. (1999a). The IKKbeta subunit of IkappaB kinase (IKK) is essential for nuclear factor kappaB activation and prevention of apoptosis. J. Exp. Med. *189*, 1839–1845.

Li, Q., Van Antwerp, D., Mercurio, F., Lee, K.F., and Verma, I.M. (1999b). Severe liver degeneration in mice lacking the IkappaB kinase 2 gene. Science *284*, 321–325.

Liston, A., Lesage, S., Wilson, J., Peltonen, L., and Goodnow, C.C. (2003). Aire regulates negative selection of organ-specific T cells. Nat. Immunol. *4*, 350–354.

Luo, J.L., Tan, W., Ricono, J.M., Korchynskyi, O., Zhang, M., Gonias, S.L., Cheresh, D.A., and Karin, M. (2007). Nuclear cytokine-activated IKKalpha controls prostate cancer metastasis by repressing Maspin. Nature *446*, 690–694.

Mathis, D., and Benoist, C. (2004). Back to central tolerance. Immunity *20*, 509–516.

Matsushima, A., Kaisho, T., Rennert, P.D., Nakano, H., Kurosawa, K., Uchida, D., Takeda, K., Akira, S., and Matsumoto, M. (2001). Essential role of nuclear factor (NF)-kappaB-inducing kinase and inhibitor of kappaB (IkappaB) kinase alpha in NF-kappaB activation through lymphotoxin beta receptor, but not through tumor necrosis factor receptor I. J. Exp. Med. *193*, 631–636.

Miyawaki, S., Nakamura, Y., Suzuka, H., Koba, M., Yasumizu, R., Ikehara, S., and Shibata, Y. (1994). A new mutation, aly, that induces a generalized lack of lymph nodes accompanied by immunodeficiency in mice. Eur. J. Immunol. *24*, 429–434.

Nagamine, K., Peterson, P., Scott, H.S., Kudoh, J., Minoshima, S., Heino, M., Krohn, K.J., Lalioti, M.D., Mullis, P.E., Antonarakis, S.E., et al. (1997). Positional cloning of the APECED gene. Nat. Genet. *17*, 393–398.

Novack, D.V., Yin, L., Hagen-Stapleton, A., Schreiber, R.D., Goeddel, D.V., Ross, F.P., and Teitelbaum, S.L. (2003). The IkappaB function of NF-kappaB2 p100 controls stimulated osteoclastogenesis. J. Exp. Med. *198*, 771–781.

Park, G.Y., Wang, X., Hu, N., Pedchenko, T.V., Blackwell, T.S., and Christman, J.W. (2006). NIK is involved in nucleosomal regulation by enhancing histone H3 phosphorylation by IKKalpha. J. Biol. Chem. *281*, 18684–18690.

Qin, J., Konno, H., Ohshima, D., Yanai, H., Motegi, H., Shimo, Y., Hirota, F., Matsumoto, M., Takaki, S., Inoue, J., and Akiyama, T. (2007). Developmental Stage-Dependent Collaboration between the TNF Receptor-Associated Factor 6 and Lymphotoxin Pathways for B Cell Follicle Organization in Secondary Lymphoid Organs. J. Immunol. *179*, 6799–6807.

Quezada, S.A., Jarvinen, L.Z., Lind, E.F., and Noelle, R.J. (2004). CD40/CD154 interactions at the interface of tolerance and immunity. Annu. Rev. Immunol. *22*, 307–328.

Ramakrishnan, P., Wang, W., and Wallach, D. (2004). Receptor-specific signaling for both the alternative and the canonical NF-kappaB activation pathways by NF-kappaB-inducing kinase. Immunity *21*, 477–489.

Rossi, S.W., Kim, M.Y., Leibbrandt, A., Parnell, S.M., Jenkinson, W.E., Glanville, S.H., McConnell, F.M., Scott, H.S., Penninger, J.M., Jenkinson, E.J., et al. (2007). RANK signals from CD4(+)3(-) inducer cells regulate development of Aire-expressing epithelial cells in the thymic medulla. J. Exp. Med. *204*, 1267–1272.

Seach, N., Ueno, T., Fletcher, A.L., Lowen, T., Mattesich, M., Engwerda, C.R., Scott, H.S., Ware, C.F., Chidgey, A.P., Gray, D.H.D., et al. (2008). The lymphotoxin pathway regulates Aire-independent expression of ectopic genes and chemokines in thymic stroma cells. J. Immunol. *180*, 5384–5392.

Shinkura, R., Kitada, K., Matsuda, F., Tashiro, K., Ikuta, K., Suzuki, M., Kogishi, K., Serikawa, T., and Honjo, T. (1999). Alymphoplasia is caused by a point mutation in the mouse gene encoding Nf-kappa b-inducing kinase. Nat. Genet. *22*, 74–77.

Theill, L.E., Boyle, W.J., and Penninger, J.M. (2002). RANK-L and RANK: T cells, bone loss, and mammalian evolution. Annu. Rev. Immunol. *20*, 795–823.

Venanzi, E.S., Gray, D.H., Benoist, C., and Mathis, D. (2007). Lymphotoxin Pathway and Aire Influences on Thymic Medullary Epithelial Cells Are Unconnected. J. Immunol. *179*, 5693–5700.

Walsh, M.C., and Choi, Y. (2003). Biology of the TRANCE axis. Cytokine Growth Factor Rev. *14*, 251–263.

Weih, F., Carrasco, D., Durham, S.K., Barton, D.S., Rizzo, C.A., Ryseck, R.P., Lira, S.A., and Bravo, R. (1995). Multiorgan inflammation and hematopoietic abnormalities in mice with a targeted disruption of RelB, a member of the NF-kappa B/Rel family. Cell *80*, 331–340.

Wong, B.R., Josien, R., Lee, S.Y., Sauter, B., Li, H.L., Steinman, R.M., and Choi, Y. (1997). TRANCE (tumor necrosis factor [TNF]-related activation-induced cytokine), a new TNF family member predominantly expressed in T cells, is a dendritic cell-specific survival factor. J. Exp. Med. *186*, 2075–2080.

Yamamoto, Y., Verma, U.N., Prajapati, S., Kwak, Y.T., and Gaynor, R.B. (2003). Histone H3 phosphorylation by IKK-alpha is critical for cytokine-induced gene expression. Nature *423*, 655–659.

Yoshida, H., Naito, A., Inoue, J., Satoh, M., Santee-Cooper, S.M., Ware, C.F., Togawa, A., Nishikawa, S., and Nishikawa, S. (2002). Different cytokines induce surface lymphotoxin-alphabeta on IL-7 receptor-alpha cells that differentially engender lymph nodes and Peyer's patches. Immunity *17*, 823–833.

Zhang, X., Wang, H., Claudio, E., Brown, K., and Siebenlist, U. (2007). A role for the IkappaB family member Bcl-3 in the control of central immunologic tolerance. Immunity *27*, 438–452.

Zhu, M., Chin, R.K., Christiansen, P.A., Lo, J.C., Liu, X., Ware, C., Siebenlist, U., and Fu, Y.X. (2006). NF-kappaB2 is required for the establishment of central tolerance through an Aire-dependent pathway. J. Clin. Invest. *116*, 2964–2971.

Zuklys, S., Balciunaite, G., Agarwal, A., Fasler-Kan, E., Palmer, E., and Hollander, G.A. (2000). Normal thymic architecture and negative selection are associated with Aire expression, the gene defective in the autoimmune-polyendocrinopathy-candidiasis-ectodermal dystrophy (APECED). J. Immunol. *165*, 1976–1983.